13

Organic Materials in Nanochemistry

Alireza Aslani
[1]*Nanobiotechnology Research Center,*
Baqiyatallah University Medical of Science, Tehran,
[2]*Department of Chemistry, Faculty of Basic Science,*
Jundi Shapur University of Technology, Dizful,
Islamic Republic of Iran

1. Introduction

At the turn of twenty-first century, we entered nanoworld. These days, if our try to run a simple web search with the keyword "nano" more than thousands and thousands of references will come out: nanoparticles, nanowires, nanostructures, nanocomposite materials, nanoprobe microscopy, nanoelectronics, nanotechnology, nanochemistry, nanomaterials and so on. The list could be endless. When did this scientific nanorevolution actually happen? Perhaps, it was in the mid-1980s, when scanning tunneling microscopy (STM) was invented. Specialists in scanning electron microscopy (SEM) may strongly object to this fact by claiming decades of experience in observing features with nearly atomic resolution and later advances in electron-beam lithography. We should not omit molecular beam epitaxy, the revolutionary technology of the 1980s, which allows producing layered structures with the thickness of each layer in the nanometer range. Colloid chemists would listen to that with a wry smile, and say that in the 1960s and 1970s, they made Langmuir-Blodgett (LB) films with extremely high periodicity in nanometer scale. From this point of view, the nanorevolution was originated from the works of Irving Langmuir and Katherine Blodgett in 1930s. What is the point of such imaginary arguments? All parties were right. We cannot imagine modern nanotechnology without any of the abovementioned contributions. The fact is that we are in the nanoworld now, and the words with prefix "nano" suddenly have become everyday reality. Perhaps it is not that important how it happened. Hence nanotechnology is a very promising field for industrial applications. In fact, several products are already on the market for certain niche sectors with high added value, e.g., biomedical materials and analytic devices. The real revolution in nanomaterial applications, however, is expected to involve widely used bulk products. Polymers like polyolefins and polyvinylchloride (PVC), for example, are good candidates in this respect because of their large-scale use and versatility. Indeed, one of the first applications of nanotechnology was the production of nanofillers for the improvement of the mechanical properties of polymers. Polypropylene (PP) is particularly interesting because of its low cost and good mechanical properties. This polymer has been used in conventional composites for a long time and, in combination with nanofillers, shows better mechanical properties with even low amounts of filler. The main nanofillers used today are nanoclay (natural product) and other nanomaterials (synthetic). Synthetic carbon nanotubes are very expensive. Nanoclays (layered silicates), in contrast, are especially interesting for bulk

applications because they are relatively inexpensive and they cause an improvement in the mechanical properties of polymers. Commonly used nanoclays include montmorillonite, hectorite, and saponite, all of which belong to the same general family of 2:1 layered or phyllosilicates. As a result of the material reduction, the environmental impact of PP nanocomposite products can be expected to be lower than that of products made out of conventional material unless the production of the nanoparticles is accompanied by particularly high environmental impacts. Nanocomposites are as multiphase materials, where one of the phases has nanoscale additives. They are expected to display unusual properties emerging from the combination of each component. According to their matrix materials, nanocomposites can be classified as ceramic matrix nanocomposites (CMNC), metal matrix nanocomposites (MMNC), and polymer matrix nanocomposites (PMNC). Polymers are now the most widely used in the field of technical textiles. The widespread use of common organic polymers such as polyolefins, polyesters and polyurethanes emanates from key features such as lightweight, easy fabrication, exceptional processability, durability and relatively low cost. A major challenge in polymer science is to broaden the application window of such materials by retaining the above features while enhancing particular characteristics such as modulus, strength, fire performance and heat resistance. However, polymers have relatively poor mechanical, thermal, and electrical properties as compared to metals and ceramics. Many types of polymers such as homopolymers, co-polymers, blended polymers and modified polymers are not sufficient enough to compensate various properties, which we have demanded. Alternative approaches to improve their properties are to reinforce polymers with inclusion of fiber, whisker, platelets or particles. The choice of the polymers is usually guided mainly by their mechanical, thermal, electrical, optical and magnetic behaviors. However, other properties such as hydrophobic-hydrophilic balance, chemical stability, bio-compatibility, opto-electronic properties and chemical functionalities have to be considered in the choice of the polymers. The polymers in many cases can also allow easier shaping and better processing of the composite materials. The inorganic particles not only provide mechanical and thermal stability, but also new functionalities that depend on the chemical nature, the structure, the size, and crystallinity of the inorganic nanoparticles (silica, transition metal oxides, metallic phosphates, nanoclays, nanometals and metal chalcogenides). Indeed, the inorganic particles can implement or improve mechanical, thermal, electronic, magnetic and redox properties, density, refractive index. Organic polymer-based inorganic nanoparticle composites have attracted increasing attention because of their unique properties emerging from the combination of organic and inorganic hybrid materials. The composites have been widely used in the various fields such as military equipments, safety, protective garments, automotive, aerospace, electronics, stabilizer and optical devices. However, these application areas continuously demand additional properties and functions such as high mechanical properties, flame retardation, chemical resistance, UV resistance, electrical conductivity, environmental stability, water repellency, magnetic field resistance and radar absorption. Moreover, the effective properties of the composites are dependent upon the properties of constituents, the volume fraction of components, shape and arrangement of inclusions and interfacial interaction between matrix and inclusion. With the recent development in the nanoscience and nanotechnology fields, the correlation of material properties with filler size has become a focal point of significant interest. On the other hand Polypropylene (PP) is one of the fastest growing commercial thermoplastics due to its attractive combination of low density and

high heat distortion temperature. There are some limitations in physico-chemical properties that restrict PP applications. A typical illustration is in packaging, where PP has poor oxygen gas barrier resistance. No single polymer has shown the ideal combination of performance features. PP possesses good water vapor barrier properties, but it is easily permeated by oxygen, carbon dioxide, and hydrocarbons. The necessity of developing more effective barrier polymers has given rise to different strategies to incorporate and optimize the features from several components. Most schemes to improve PP gas barrier properties involve either addition of higher barrier plastics via a multilayer structure (co-extrusion) or by introducing filler with high aspect ratio in the polymer matrix. Co-extrusion allows tailoring of film properties through the use of different materials where each material component maintains its own set of properties, compared with blending of polymers in a mono-extrusion technique. Co-extrusion is used to generate multilayer laminate structures from separately extruded polymer films that are sandwiched together. Resulting films may comprise many layers, such as the PP-adhesive poly (ethylene-co-vinyl alcohol) (EVOH)-adhesive PP system: EVOH barrier sheet trapped between two layers of moisture resistant PP and two additional adhesive strata. However, by nature co-extrusion is a complex and expensive process. Alternatively, nano fillers with high aspect ratio can be loaded into the polymer matrix. Polymer nanocomposites are a better choice with significant property increments from some materials. Nanocomposite materials are one of the methods for improving gas barrier properties of polyolefin. Recent developments in polymer nanocomposites have attracted attention due to the possibilities offered by this technology to enhance the barrier properties of inexpensive commodity polymers. Many studies have demonstrated improvements in permeability reduction to gases, moisture and organic vapors resulting from the addition of low concentrations of layered some nanoparticles to various thermoplastic matrices. This is mainly due to their nanometer scale particle size and intraparticle distances. The desired properties are usually reached at low filler volume fraction, allowing the nanocomposites to retain macroscopic dispersion and low density of the polymer. The geometrical shape of the particle plays an important role in determining the properties of the composites. The improved nanocomposite barrier behavior illustrated by many examples has been explained by the tortuous path model, in which the presence of impermeable some platelets generates an overlapped structure that hinders penetrate diffusion and thus decreases the permeability of the material.

2. Nanotechnology

Nanotechnology is receiving a lot of attention of late across the globe. The term nano originates etymologically from the Greek, and it means "dwarf." The term indicates physical dimensions that are in the range of one-billionth (10^{-9} or $\frac{1}{10^9}$) of a meter. This scale is called colloquially nanometer scale, or also nanoscale. One nanometer is approximately the length of two hydrogen atoms. Nanotechnology relates to the design, creation, and utilization of materials whose constituent structures exist at the nanoscale; these constituent structures can, by convention, be up to 100 nm in size. Nanotechnology is a growing field that explores electrical, optical, and magnetic activity as well as structural behavior at the molecular and sub-molecular level. These questions should be answered: What is nanotechnology? What are the applications of nanotechnology? What is the market potential for nanotechnology? What are the global research activities in nanotechnology? Why would a practitioner, need to care?

Research and technology development at the atomic, molecular, or macromolecular levels, in the length scale of approximately 1 to 100 nm range called nanotechnology. Creating and using structures, devices, and systems that have novel properties and functions because of their small and/or intermediate size are application of nanomaterials. Hence, nanotechnology can be defined as the ability to work at the molecular level, atom by atom, to create large structures with fundamentally new properties and functions. Nanotechnology can be described as the precision-creation and precision-manipulation of atomic-scale matter; hence, it is also referred to as precision molecular engineering.

Nanotechnology is the application of nanoscience to control processes on the nanometer scale that is, between 1 to 100 nm or call better 2 to 50 nm. The field is also known as molecular engineering or molecular nanotechnology (MNT). MNT deals with the control of the structure of matter based on atom-by-atom and/or molecule-by-molecule engineering; also, it deals with the products and processes of molecular manufacturing. The term engineered nanoparticles describes particles that do not occur naturally; humans have been putting together different materials throughout time, and now with nanotechnology they are doing so at the nanoscale. As it might be inferred, nanotechnology is highly interdisciplinary as a field, and it requires knowledge drawn from a variety of scientific and engineering arenas: Designing at the nanoscale is working in a world where physics, chemistry, electrical engineering, mechanical engineering, and even biology become unified into an integrated field. "Building blocks" for nanomaterials include carbon-based components and organics, semiconductors, metals, and metal oxides; nanomaterials are the infrastructure, or building blocks, for nanotechnology. The term nanotechnology was introduced by Nori Taniguchi in 1974 at the Tokyo International Conference on Production Engineering. He used the word to describe ultrafine machining: the processing of a material to nanoscale precision. This work was focused on studying the mechanisms of machining hard and brittle materials such as quartz crystals, silicon, and alumina ceramics by ultrasonic machining. Years earlier, in a lecture at the annual meeting of the American Physical Society in 1959 (There's Plenty of Room at the Bottom) American Physicist and Nobel Laureate Richard Feynman argued (although he did not coin or use the word nanotechnology) that the scanning electron microscope could be improved in resolution and stability, so that one would be able to "see" atoms. Feynman proceeded to predict the ability to arrange atoms the way a researcher would want them, within the bounds of chemical stability, in order to build tiny structures that in turn would lead to molecular or atomic synthesis of materials. Based on Feynman's idea, K. E. Drexler advanced the idea of "molecular nanotechnology" in 1986 in the book Engines of Creation, where he postulated the concept of using nanoscale molecular structures to act in a machinelike manner to guide and activate the synthesis of larger molecules. Drexler proposed the use of a large number (billions) of robotic-like machines called "assemblers" (or nanobots) that would form the basis of a molecular manufacturing technology capable of building literally anything atom by atom and molecule by molecule. At this time, an engineering discipline has already grown out of the pure and applied science; however, nanoscience still remains somewhat of a maturing field. Nanotechnology can be identified precisely with the concept of "molecular manufacturing" (molecular nanotechnology) introduced above or with a broader definition that also includes laterally related sub-disciplines. The nanoscale is where physical and biological systems approach a comparable dimensional scale. A basic "difference" between systems biology and nanotechnology is the goal of the science: systems biology aims to

uncover the fundamental operation of the cell in an effort to predict the exact response to specific stimuli and genetic variations (has scientific discovery focus); nanotechnology, on the other hand, does not attempt to be so precise but is chiefly concerned with useful design.

A nanometer is about the width of four silicon atoms (with a radius of 0.13 nm) or two hydrogen atoms (radius of 0.21 nm); .For comparison purposes, the core of a single-mode fiber is 10.000 nm in diameter, and a 10 nm nanowire is 1000 times smaller than (the core of) a fiber. The nanoscale exists at a boundary between the "classical world" and the "quantum mechanical world"; therefore, realization of nanotechnology promises to afford revolutionary new capabilities.

The nanoparticles are ultrafine particles in the size of nanometer order. "Nano" is a prefix denoting the minus 9th power of ten, namely one billionth. Here it means nanometer (nm) applied for the length. One nm is extremely small length corresponding to one billionth of 1 m, one millionth of 1 mm, or one thousandth of 1 μm. The definition of nanoparticles differs depending upon the materials, fields and applications concerned. In the narrower sense, they are regarded as the particles smaller than 10 to 20 nm, where the physical properties of solid materials themselves would drastically change. On the other hand, the particles in the three digit range of nanometer from 1 nm to 1μm could be called as nanoparticles. In many cases, the particles from 1 to 100 nm are generally called as nanoparticles, but here they will be regarded as the particles smaller than those called conventionally "submicron particles", and concretely less than the wavelength of visible light (its lower limit is about 400 nm) as a measure, which need to be treated differently from the submicron particles.

3. Features of nanoparticles: "Activation of particle surface"

All the solid particles consist of the atoms or the molecules. As they are micronized, they tend to be affected by the behavior of atoms or the molecules themselves and to show different properties from those of the bulk solid of the same material. It is attributable to the change of the bonding state of the atoms or the molecules constructing the particles. The diameter of the smallest hydrogen atom is 0.074 nm, and that of the relatively large lead atom (atomic number is 82) is 0.35 nm. From these sizes, it is estimated that the particle with a size of 2 nm consists of only several tens to thousands atoms. When the particle is constructed by larger molecules, the number decreases furthermore [M. Arakawa, 2005[a] and 1983[b]]. It is indicated that the fraction of surface atoms of a 20 μm cubic particle is only 0.006%, but it increases to 0.6% for a 200 nm particle and then it is estimated almost half of the atoms are situated at the surface of a 2 nm particle. On the other hand, as the micronization of solid particles, the specific surface area increases generally in reversal proportion to the particle size. In the above-mentioned case, when the particle of 1cm is micronized to 1 μm and 10 nm, the specific surface area becomes ten thousand times and million times, respectively. As the increase in the specific surface area directly influences such properties like the solution and reaction rates of the particles, it is one of major reasons for the unique properties of the nanoparticles different from the bulk material together with the change in the surface properties of the particles itself.

4. Evaluation of size of nanoparticles

In order to elucidate the change in properties and characteristics of nanoparticles with the particle size, it is essential first of all to measure the size of the nanoparticles accurately. The

most basic method to measure the size of nanoparticles is the size analysis from the picture image using the transmission electron microscope, which could also give the particle size distribution. For this analysis, preparation of the well-dispersed particles on the sample mount is the key issue. The grain size of the particles can be obtained from peak width at half height in the X-ray diffraction analysis and it is regarded as an average primary particle size of particles. Meanwhile, the laser diffraction and scattering method, which is popular for the size analysis of micron-sized particles, would hardly measure the particle size of individual nanoparticles but that of the agglomerated particles. The photon correlation method often used for the particle analysis in the nanosized range might not give accurate results in many cases, when the particle size distribution is wide. Then the BET (Brunauer-Emmett-Teller) specific surface measurement based on the gas adsorption is often applied as a simple method to evaluate the size of nanosized primary particles. By this method, it is possible to estimate the particle size from the specific surface area under the assumption of spherical particle shape. This equivalent particle size based on the specific surface area is useful for the evaluation of nanoparticle size, though it may differ from the particle size observed by the electron microscope depending upon the surface state and the inner structure of the particles.

5. Properties of nanoparticles and size effect

As mentioned above, with the decreasing particle size, the solid particles generally tend to show different properties from the bulk material and even the physical properties like melting point and dielectric constant themselves which have been considered as specific properties may change, when the particles become in several nanometer size. These changes in the fundamental properties with the particle size are called “size effect” in a narrower sense. On the contrary, in a broader sense, it could also include the change in the various characteristics and behaviors of particles and powders with the particle size. The nanoparticles have various unique features in the morphological/structural properties, thermal properties, electromagnetic properties, optical properties, mechanical properties as described briefly in the following:

5.1 Morphological and structural properties

The ultrafine size of the nanoparticles itself is one of useful functions. For example, the finer particles are apt to be absorbed more easily through the biological membrane. It is known as the enhanced permeation and retention (EPR) effect [H. Maeda, 1992] that the particles having a particle size from about 50 to 100 nm, which would not be transferred to the normal cells through the vascular wall could be delivered selectively to a certain affected cells because of the enlarged cell gap of this part. As mentioned above, the large specific surface area of the nanoparticles is an important property to the reactivity, solubility, sintering performance etc. related with the mass and heat transfer between the particles and their surroundings from the morphological viewpoint apart from the control of the surface and inner structures of the nanoparticles. Furthermore, the crystal structure of the particles may change with the particle size in the nanosized range in some cases. Uchino et al. [K. Uchino, 1982] reported that from the X-ray diffraction analysis of the lattice constant of $BaTiO_3$ powder prepared by hydrothermal synthesis method, the c/a axis length ratio showing the tetragonal characteristics decreased to indicate the increasing symmetric

property with the decreasing particle size from about 200 nm as shown in fig 1. This is considered to be attributable to the compressive force exerted on the particles as a result of the surface tension of the particle itself. For $PbTiO_3$, it is reported that the tetragonal crystals decreased and the cubical crystal increased in the particles from the particle size of about 18 nm [H. Suzuki, 2002]. In this way, the critical particle size for the crystal structure and the size effect differ with the materials concerned.

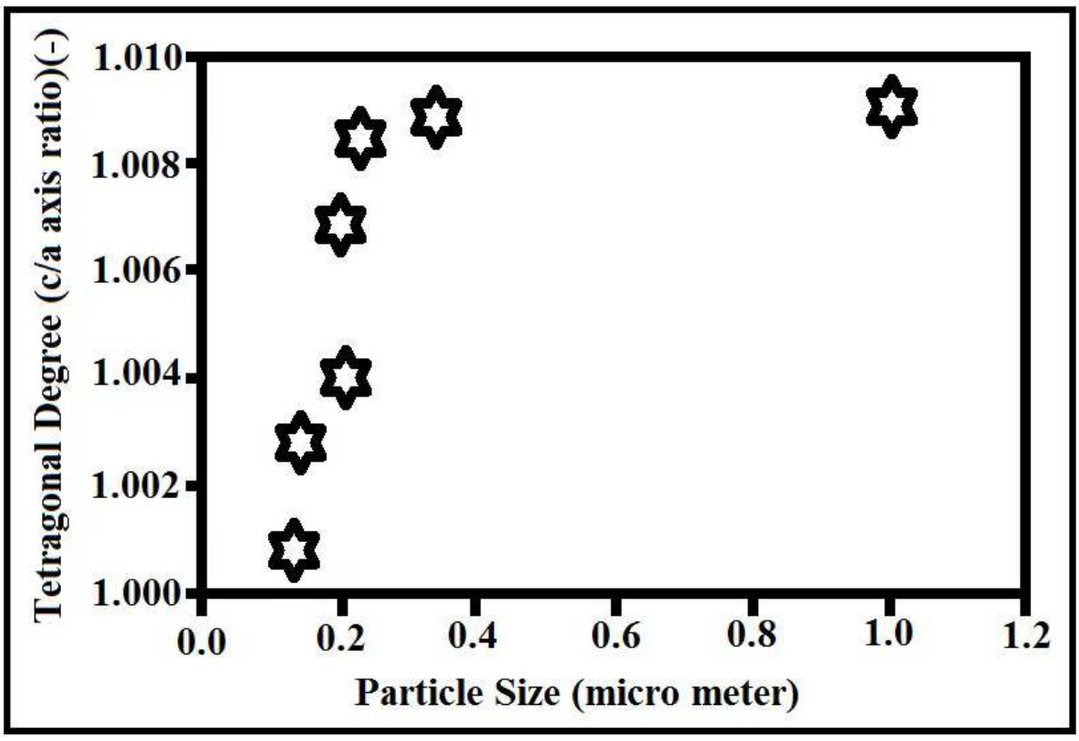

Fig. 1. Relationship between particle size and tetragonal degree (c/a axis ratio) of $BaTiO_3$ powder.

5.2 Thermal properties

As the atoms and molecules located at the particle surface become influential in the nanometer order, the melting point of the material decreases from that of the bulk material because they tend to be able to move easier at the lower temperature. For example, the melting point of gold is 1336 K as a bulk but starts to decrease remarkably below the particle size of about 20 nm and drastically below 10 nm and then becomes more than 500 degrees lower than that of the gold bulk around 2 nm. The reduction of the melting point of ultrafine particles is regarded as one of the unique features of the nanoparticles related with aggregation and grain growth of the nanoparticles or improvement of sintering performance of ceramic materials [N. Wada, 1984].

5.3 Electromagnetic properties

The nanoparticles are used as the raw material for a number of electronic devices. The electric properties and particle size of these nanoparticles play a great role for the

improvement of the product performance [I. Matsui, 2005]. As an example, there is a strong demand for the materials with a high dielectric constant to develop small and thin electronic devices. For this purpose, it has been confirmed by the X-ray diffraction analysis for instance that the dielectric constant of $PbTiO_3$ tends to increase considerably as the particles become smaller than about 20 nm. Meanwhile, it is also known that when the dielectric constant is measured with a pellet prepared by pressing these nanoparticles, it shows a peak with the raw material around 100nm and decreases with the decreasing particle size, which is attributable to the influence of the grain boundary and void in the pellet [M. Takashige, 1981].

On the other hand, the minimum particles size to keep the ferroelectric property (critical size) differs depending upon the kind and composition of the materials. Summarizing the data of various kinds of materials, it varies from 7 nm for $PbTiO_3$ to 317 nm for Ba–Pb–Ti compounds. The Curie point defined as the point changing from the ferroelectric material to the paraelectric phase of $PbTiO_3$ reduces drastically with the decreasing particle size below 20–30 nm as shown in fig 2. As for the Curie point, some equations have been proposed for its estimation [K. Ishikawa, 2001].

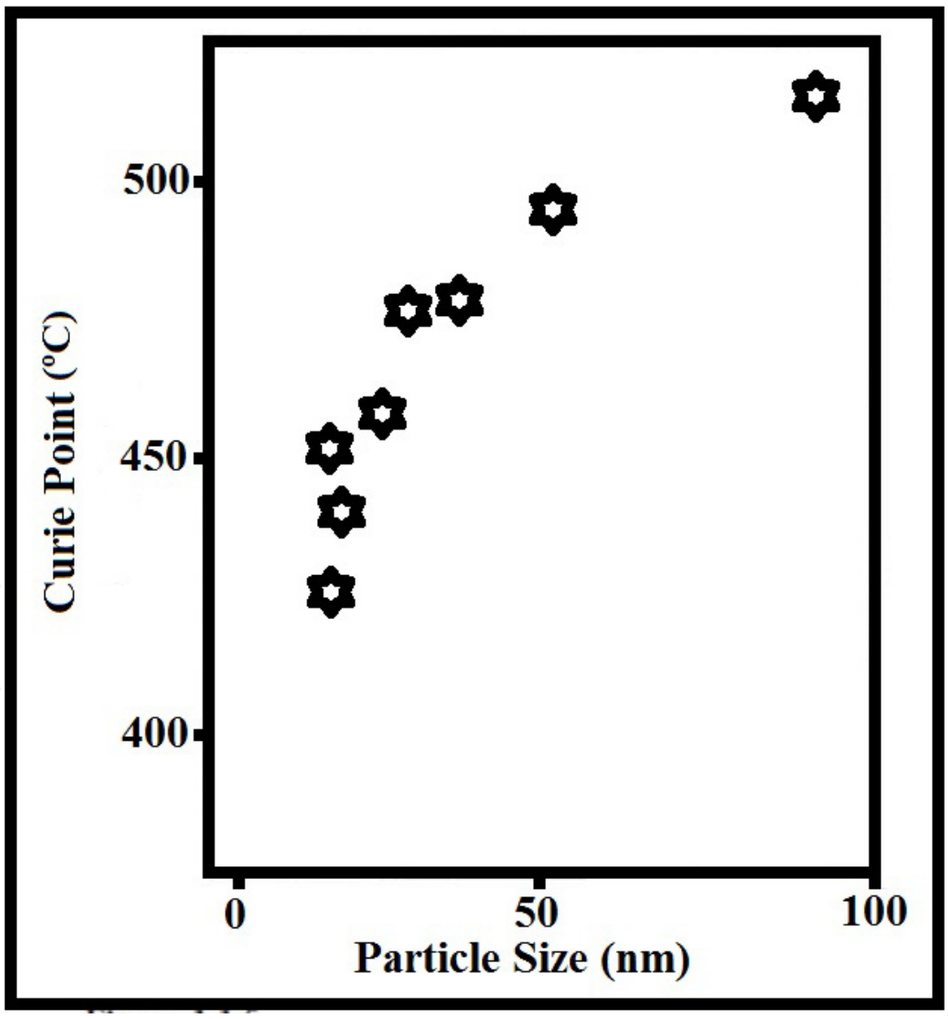

Fig. 2. Change of Curie point of $PbTiO_3$ with its particle size.

As for the magnetic property, ferromagnetic fine particles have a single magnetic domain structure as they become very small as in the order less than about 1 μm and show super-paramagnetic property, when they get further finer. In this case, although the individual particles are ferromagnetic with the single magnetic domain structure, the particles collectively behave as a paramagnetic. It is magnetized as a whole in the same direction of the external magnetic field but the magnetization disappears by the thermal fluctuation, when the external magnetic field is taken away. The time for disappearing of magnetization depends upon the particle size, namely the magnetization of the material responds promptly with the external magnetic field as a paramagnetic when the particles are small enough but it decreases gradually as the particle size becomes larger. As a result of such change in the electromagnetic properties of nanoparticles, it is known for instance that the gold which is a stable substance as a bulk shows unique catalytic characteristics as nanoparticles [K. Ishikawa, 1998 and M. Haruta, 1994].

5.4 Optical properties

As the size of particles becomes in the several nanometers range, they absorb the light with a specific wavelength as the plasmon absorption [Y. Kurokawa, 1996] caused by the plasma oscillation of the electrons and the transmitted light with different color depending upon the kind of metal and particle size is obtained [K. Kobayashi, 2004 and S. Sato, 1996].

In case of gold nanoparticles, it is reported that the maximum light absorption wavelength is 525 nm for the particles of 15nm but it is enlarged by about 50 nm for 45 nm particles. In this way, these gold and silver nanoparticles show the color phenomena with splendid tinting strength, color saturation and transparency compared with the conventional pigments for the paint in the submicron size and the tinting strength per unit volume of silver nanoparticles becomes about 100 times higher than that of organic pigments. Furthermore, since the nanoparticles are smaller than the wavelength of visible light and the light scattering by the particles becomes negligible, higher transparency can be obtained with the nanoparticles than the conventional pigment.

5.5 Mechanical properties

It is known that the hardness of the crystalline materials generally increases with the decreasing crystalline size and that the mechanical strength of the materials considerably increases by micronizing the structure of the metal and ceramic material or composing them in the nano range [K. Niihara, 1991 and T. Sekino, 2000]. Furthermore, with the ceramic material having crystalline size less than several hundred nanometers, the unique super-plastic phenomenon is seen that it is extended several to several thousand times from the original size at the elevated temperature over 50 % of the melting point [F. Wakai, 1990], which may provide the possibility of forming and processing of ceramics like metallic materials.

6. Existing conditions of particles and their properties

The nanoparticles usually exhibit collective functions. Therefore, the dispersing state and the surrounding conditions in addition to the physical properties of the particles themselves are important. In many cases, the nanoparticles exist as aggregates of the primary particles

by the adhesion and bonding during the production process because of their high adhesiveness. The existing state of the nanoparticles is greatly influenced by the surrounding conditions if they are in gas, liquid, solid or in a vacuum and what sort of interaction they have with the surrounding materials. The nanoparticles are rarely used by themselves but dispersed in other materials or combined with them. The dispersing process of the nanoparticles is a key for the nanoparticle technology as well as their preparation methods, since the performance of the final products are affected by their dispersing conditions [T. Yokoyama, 2005]. In this way, it is expected with great possibility to develop various new materials and applications by the nanoparticle technology producing and processing the nanoparticles, which have different properties from the bulk material by the size effects as mentioned above and in the following sections.

7. Wet technologies for the formation of organic nanostructures

Chemical methods of material processing were known for years, existing in parallel with physical and other methods of film deposition. Recent advances in electron microscopy and scanning nanoprobe microscopy (STM, AFM) have revealed that some of the materials produced by the chemical methods have distinctive nanocrystalline structure. Furthermore, due to the achievements of colloid chemistry in the last 20 years, a large variety of colloid nanoparticles have become available for film deposition. This has stimulated great interest in further development of chemical methods as cost-effective alternatives to such physical methods as: thermal evaporation; magnetron sputtering; chemical and physical vapor deposition (CVD, PVD); and molecular beam epitaxy (MBE).

7.1 Formation of colloid nanoparticles

The most advanced chemical method for nano-structured materials processing is the deposition of colloid inorganic particles. Recent achievements in colloid chemistry have made a large variety of colloid compounds commercially available. The list of colloid nanoparticles with uniform (low-dispersed) dimensions in the range from 3 to 50 nm includes the noble metals (e.g., Au, Ag, Pt, Pd, and Cu), semiconductors (e.g., Si, Ge, III-V and II-VI, and metal oxides), insulators (e.g., mica, silica, different ceramic materials, polymers), and magnetic materials (e.g, Fe_2O_3, Ni, Co, and Fe). The growth of colloid particles is usually stabilized during synthesis by adding surfactants to the reagents [Edelstein. A. S. 1996]. Therefore, the stable nanoparticles produced are coated with a thin shell of functionalized hydrocarbons, or some other compounds. Typical examples of the chemistry of formation of colloid nanoparticles are shown below. Gold stable colloids can be prepared by the reduction of $AuCl_4$ with sodium borohydride in the presence of alkane-thiols [Brust. M, 1994]. Other colloids, such as Ag, CdS, CdSe, and ZnS, can be prepared in a similar way. InP nanocrystals can be synthesized by the following reaction, with temperatures ranging from 150 °C to 280 °C in the presence of either primary amines, tri-*n*-octylphosphine (TOP), or tri-*n*-octylphosphine oxide (TOPO) as stabilizing agents, preventing further InP aggregation [Talapin. D. V, 2002].

$$InCl_3 + [(CH_3)_3Si]_3P \rightarrow InP + 3(CH_3)_3SiCl$$

The particles appear to be mono-dispersed, with a mean cluster size varying from 2 to 6 nm depending on the stabilizer used. The particles show strong resonance luminescence after

etching in HF. Cobalt mono-dispersed nanocrystals can be produced by rapid pyrolysis of the organic precursor $Co(CO)_8$ in an inert Ar-atmosphere, and in the presence of organic surfactants, such as oleic-acid and trioctylphosphonic acid at high temperatures [Puntes. V. F., 2001]. The particles appear to have ideal spherical, cubical, or rod-like shapes, with sizes in the range from 3 to 17 nm depending on surfactant concentration. The Co nanoparticles demonstrate superparamagnetic ferromagnetic transition. CdTe nanoparticle colloids can be prepared by the reaction of Na_2Te with CdI_2 in methanol at –78 °C.

The diameter of CdTe colloid particles is in the range from 2.2 to 2.5 nm [Schultz. D. L, 1996]. An alternative method for the formation of stabilized colloid particles is to utilize self-assembled membranes, such as micelles, microemulsions, liposomes, and vesicles. Typical dimensions are from 3 to 6 nm for reverse micelles in aqueous solutions, from 5 to 100 nm for emulsions, and from 100 to 800 nm for vesicles. Liposomes are similar to vesicles, but they have bilayer membranes made of phospholipids. Such membranes may act as the reaction cage during the formation of nanoparticles, and may prevent their further aggregation. The idea of the formation of nanoparticles inside micelles is to trap respective cations there. This can be done by sonification of the mixture of required salts and surfactants. Since the permeability of the membrane for anions is about 100 times higher than for cations, the formation of nanoparticles takes place within micelles, with a constant supply of anions from outside. A number of different colloids, such as CdSe, Ag_2O, Fe_2O_3, Al_2O_3, and cobalt ferrite, were prepared using the above methods [Bhandarkar. S, 1990, Mann. S, 1983, Mann. S. J. P, 1986, Cortan. A. R, 1990, Yaacob. I. I, 1993, and Li. S, 2001].

7.2 Self-assembly of colloid nanoparticles

The deposition of colloid nanoparticles onto solid substrates can be accomplished by different methods, such as simple casting, electrostatic deposition, Langmuir-Blodgett, or spin coating techniques. However, the simplest method of nanoparticles deposition, which gives some remarkable results, is the so-called self-assembly or chemical self-assembly method. This method, which was first introduced by Netzer and Sagiv, is based upon strong covalent bonding of the adsorbed objects (i.e., monomer or polymer molecules and nanoparticles) to the substrate via special functional groups. It is known, for example, that the compounds containing thiol (SH) or amine (NH_2) groups have strong affinity to gold. The silane group (SiH_3) with silicon is another pair having very strong affinity.

The first work on the self-assembly of gold colloid particles capped with alkanethiols was done by Brust and coworkers [Netzer, L, 1983]. This routine has been adopted by other scientists for the deposition of self-assembled monolayers of different colloid nanoparticles (e.g., Ag, CdS, CdSe, and ZnS), which were prepared using mercapto-alcohols, mercaptocarboxylic acids, and thiophenols as capping agents. Self-assembled nanoparticles usually show well-ordered lateral structures, proved by numerous observations with SEM, STM, and AFM [Collier. C, 1997, Lover. T, 1997, Rogach. A. L, 1999 and Vogel. W, 2000].

Two-dimensional ordering in self-assembled nanoparticle monolayers can be substantially improved by thermal annealing at temperatures ranging from 100 °C to 200 °C, depending on the material used. The use of bi-functional $HS-(CH_2)_{10}-COOH$ bridging molecules, which combines both the affinity of thiol groups to gold and carboxylic group to titania, can provide more flexibility in the self-assembly. Both self-assembly routes were exploited for

deposition of TiO_2 nanoparticles onto the gold surface [Rizza. R, 1997]. In the first one, unmodified TiO_2 nanoparticles were self-assembled onto the gold surface, coated with a monolayer of HS-$(CH_2)_{10}$-COOH; while in the second one, TiO_2 nanoparticles stabilized with HS-$(CH_2)_{10}$-COOH were self-assembled onto the bare gold surface. For some time, chemical self-assembly was limited to the formation of organized monolayers. The use of bi-functional bridge molecules overcomes this relative disadvantage. For example, multi-layers of Au colloid particles can be deposited using di-thiol spacing layers. A similar routine was applied for the fabrication of Au/CdS super lattices [Sarathy. K. V, 1999 and Nakanishi. T, 1998].

7.3 Morphology and crystallography of nanostructured materials prepared by chemical routes

The structural study of materials was always of a high priority, because the physical properties of materials depend very much on their structure. There are several levels of structural study, which start with the investigation of the morphology of the material surfaces, closely related to their in-plane ordering. Many nano-structured materials prepared with the help of layer-by-layer deposition techniques, such as LB or electrostatic self-assembly, have a distinctive periodicity in the direction normal to the surface, which determines their main electrical and optical properties. This is why the study of the layer-by-layer structure of such materials is of crucial importance.

The materials consisting of colloid nanoparticles have a tendency to form two dimensional structures according to the close packing order. This trend can stimulate the formation of multilayered quasi-3D structures of closely packed nanoparticles. The final stage of structural study is the crystallography of individual nanoparticles, clusters, and grains of materials. This is a very interesting and important subject, since the crystallography of nanoclusters, which consist of several hundred to several thousand atoms, is very often different from that of their respective bulk materials.

The planar order of nanostructures deposited by chemical routes has become an important issue, because of the competition with solid-state nanotechnology capable of the fabrication of fine two-dimensional structures. The main concern is with the layers of nanoparticles produced by chemical self-assembly, because methods of electrostatic self-assembly and LB is not capable of producing two-dimensional ordered arrays of nanoparticles. The features of the lateral arrangement of particles, which are buried under layers of either closely packed amphiphilic compounds or polymers, are usually smeared and difficult to observe. In the case of relatively thick (quasi-3D) films, produced by electrodeposition and sol-gel techniques, the morphology study usually reveals polycrystallites. Therefore, the quality of these materials can be assessed by the size of the crystallites and by the presence of preferential orientation, which may cause anisotropy of the electrical and optical properties of materials.

7.4 Morphology and crystallography of chemically self-assembled nanoparticles

In contrast to the previous deposition techniques (i.e., LB and electrostatic self-assembly), nanoparticles, which are chemically self-assembled onto the solid substrates, tend to form regular two-dimensional structures, especially after annealing at moderate temperatures.

The type of two-dimensional structure, which usually follows the trend of close packing arrangement, depends on the particles' shapes. For example, a simple hexagonal pattern is formed by spherical nanoparticles. A classic example of such structures is gold colloid particles chemically self-assembled onto the surface of gold via thiol groups. The observation of such structures is possible with scanning nanoprobe microscopy, such as STM and AFM, as well as with TEM and high resolution SEM [49-73][Roberts.G. G, 1983[a], 1990[b] and 1985[c], Ross. J, 1986, Lvov. Y. M, 1987[a], 1989[b] and 1994[c], 2000[d], Petty. M. C, 1990[a] and 1995[b], Ulman. A, 1991[a] and 1995[b], Wegner. G, 1993, Yarwood. J, 1993, Tredgold. R. H, 1994, Tsukruk. V. V, 1997, Bliznyuk. V. N, 1998, Bonnell. D. A, 2001, Stefanis. A, 2001, Gabriel. B. L, 1985, Keyse. R. J, 1998, Greffet. J. J, 1997, Kitaigorodski. A. L, 1961, Nabok.A. V, 1998[a] and 2003[b]].

8. Elemental and chemical composition of organic/inorganic nanostructures

8.1 Stabilization of colloidal metal particles in liquids

Before beginning a description of synthetic methods, a general and crucial aspect of colloid chemistry should be considered, and that is the means by which the metal particles are stabilized in the dispersing medium, since small metal particles are unstable with respect to agglomeration to the bulk. At short inter-particle distances, two particles would be attracted to each other by van-der-Waals forces and in the absence of repulsive forces to counteract this attraction an unprotected sol would coagulate. This counteraction can be achieved by two methods, electrostatic stabilization and steric stabilization. In classical gold sols, for example, prepared by the reduction of aqueous $[AuC1_4]^-$ by sodium citrate, the colloidal gold particles are surrounded by an electrical double layer formed by adsorbed citrate and chloride ions and cations which are attracted to them. This results in a Columbic repulsion between particles. The weak minimum in potential energy at moderate interparticle distance defines a stable arrangement of colloidal particles which is easily disrupted by medium effects and, at normal temperatures, by the thermal motion of the particles.

Thus, if the electric potential associated with the double layer is sufficiently high, electrostatic repulsion will prevent particle agglomeration, but an electrostatically stabilized sol can be coagulated if the ionic strength of the dispersing medium is increased sufficiently. If the surface charge is reduced by the displacement of adsorbed anions by a more strongly binding neutral adsorbate, the colloidal particles can now collide and agglomerate under the influence of the van-der-Waals attractive forces [J. S. Bradley, 1993]. Even in organic media, in which electrostatic effects might not normally be considered to be important, the development of charge has been demonstrated on inorganic surfaces, including metals, in contact with organic phases such as solvents and polymers. For example, the acquisition of charge by gold particles in organic liquids has been demonstrated, and the sign and magnitude of the charge has been found to vary as a function of the donor properties of the liquid [M. E. Labib, 1984]. Thus, even for colloidal metals in suspension in relatively non-polar liquids, the possibility cannot be excluded that electrostatic stabilization contributes to the stability of the sol.

A second means by which colloidal particles can be prevented from aggregating is by the adsorption of molecules such as polymers, surfactants or ligands at the surface of the particles, thus providing a protective layer. Polymers are widely used, and it is obvious that

the protectant, in order to function effectively, must not only coordinate to the particle surface, but must also be adequately solvated by the dispersing fluid - such polymers are termed amphiphilic. The choice of polymer is determined by consideration of the solubility of the metal colloid precursor. The solvent of choice and the ability of the polymer to stabilize the reduced metal particles in the colloidal state. Natural polymers such as gelatin and agar were often used before the advent of synthetic polymer chemistry, and related stabilizers such as cellulose acetate, cellulose nitrate [A. Duteil, 1993], and cyclodextrins [M. Komiyama, 1983] have been used more recently. Thiele [V. H. Thiele, 1965] proposed the Protective Value as a measure of the ability of a polymer to stabilize colloidal metal. It was defined, similarly to the older Gold Number of Zsigmondy. as the weight of the polymer which would stabilize 1 g of a standard red gold sol containing 50 mg/L gold against the coagulating effect of 1% sodium chloride solution. Several other studies have been performed on the relative ability of polymers to act as steric stabilizers [P. H. Hess, 1966, H. Hirai, 1979[a] and 1985[b]], and, despite the fact that these quite subjective studies focus on very specific (and quite different) sol systems, it seems that; of the synthetic polymers considered, vinyl polymers with polar side groups such as poly(vinylpyrro1idone) (PVP) and poly(viny1 a1cohole) are especially useful in this respect. The use of copolymers introduces another degree of variability to colloidal stabilization. As the co-monomer ratio can be varied. For example, the use of vinyl-pyrrolidone-vinyl-alcohol copolymers is reported for the preparation of platinum and silver hydrosols [K. Megure, 1988]. The silver sols were stable only in the presence of the copolymer, and the size of the silver particles decreased with an increase in vinyl-pyrrolidone content of the copolymer. Electrostatic and steric stabilization are in a sense combined in the use of long chain alkyl-ammonium cations and surfactants, either in single-phase sols or in reverse micelle synthesis of colloidal metals. A new class of metal colloids has recently been established in which the surface of the particle is covered by relatively small ligand molecules such as sulfonated triphenylphosphine or alkane-thiols.

8.2 Synthetic methods for the preparation of colloidal transition metals

The synthetic methods which have been used include modern versions of established methods of metal colloid preparation such as the mild chemical reduction of solutions of transition metal salts and complexes and newer methods such as radiolysis and photochemical reduction, metal atom extrusion from labile organometallics. And the use of metal vapor synthesis techniques. Some of these reactions have been in use for many years, and some are the results of research stimulated by the current resurgence in metal colloid chemistry. The list of preparative methods is being extended daily, and, as examples of these methods are described below, the reader will quickly be made aware that almost any organometallic reaction or physical process which results in the deposition of a metal is in fact a resource for the metal colloid chemist. The acquisition of new methods requires only the opportunism of the synthetic chemist in turning a previously negative result into a synthetic possibility.

8.3 The role of surfactants in nanomarerials synthesis

For over 2000 years, humankind has used surfactants or surface-active ingredients in various aspects of daily life, for washing, laundry, cosmetics, and housecleaning.

However, the development of more economical processes for the manufacture of surfactants has contributed to an increased consumption of synthetic detergents. However, the major surfactants common (with respect to detergent) to all regions are linear alkyl benzene sulfonates (LASs), alcohol ether sulfates (AESs), aliphatic alcohols (AEs), alcohol sulfates (ASs), and soap. In the past decades, new surfactants have proliferated mainly as nonionic or non-soap surfactants offering unique properties and features to both industrial and household markets. Non-soap surfactants are widely used in diverse applications such as detergents, paints, and in the cosmetics, stabilized and synthesis of new materials and pharmaceutical industries. Since the 1960s, biodegradability and a growing environmental awareness have been the driving forces for the introduction of new surfactants. These forces continue to grow and influence the surfactant market and production. A new class of surfactants, carbohydrate-based surfactants, has gained significant interest and increased market share. Consequently, sugar-based surfactants, such as alkyl-poly-glycoside (APG), are used as a replacement for poly-oxy-ethylene alkyl phenols (APEs) where biodegradability is a concern. They represent a new concept in compatibility and care. Nonetheless, over 40 different types of surfactants are produced and used commercially in the formulation of home care, personal care, and industrial products. Contrary to many textbooks that elaborate on surfactant physical properties or formulation guidelines. Surfactants are primarily anionic, nonionic, cationic, and amphoteric.

8.4 "Surfactant systems"– Structure

The interactions between the hydrophilic head-groups and the hydrophobic tail of the surfactants, they tend to form aggregates spontaneously when placed into water, oil, or a mixture of the two. The aggregates are thermodynamically stable and therefore long lived. This interaction can be represented by a geometric packing parameter. Because the head-groups of surfactants are either hydrated or charged, they prefer to maintain a certain distance from their nearest neighbors, which is represented by the area, a_0. Tail interactions, from energy and enthalpy differences between the solvent and the environment of hydrophobic tails, lead to another area based on the length and volume of the tail, v/lc. The packing parameter is the ratio of these two areas ($P = v/a_0l$c). For certain values of P, the surfactant packs into different preferred geometries, which are shown in fig 3. Normal phases (fig 3 a-c), where water is continuous, have packing parameters less than one, and reverse phases (fig 3d and 3e), where oil is continuous, have packing parameters greater than one. When spheres (fig 3a) are in random order, the system is called a micellar solution. If the spheres close pack into a lattice, a discrete cubic liquid crystal can be formed. As the packing parameter is increased, cylinders (fig 3b) are formed. In dilute solution when the orientation of the cylinders is random (i.e., uncorrelated), they are called rodlike micelles, but when close packed into a lattice, they form a hexagonal liquid crystal. Bilayer sheets (fig 3c) can give many structures. When P is close to one, the bilayers are parallel to each other and form the lamellar liquid crystal. If the packing parameter is less than one, these sheets can no longer remain parallel to each other and may fold back on themselves, trapping solvent in a bilayer container called a vesicle. The bilayers may also maintain a curved shape and fill space by following an infinite periodic minimal surface, IPMS. IPMS are a geometry that is periodic in three directions and has constant mean curvature. When the bilayer conforms to this geometry,

both the water and oil fractions are continuous in three directions, and because the IPMS give a cubic crystal pattern, these liquid crystals are known as bicontinuous cubic liquid crystals. The packing of bicontinuous cubics as well as all liquid crystals is thermodynamically controlled, so the structures conform to a regular array of fixed size. Once past the value $P = 1$, the geometries and ordered phase repeat in reverse order but with the oil and solvated surfactant tails becoming the continuous phase, i.e., reverse phases. Along with the ordered liquid crystal structures there are random geometries that are also thermodynamically stable. These systems are called micro-emulsions. They are related to regular emulsions in that they are dispersions of two immiscible liquids stabilized by surfactants. Unlike emulsions, micro-emulsions are thermodynamically stable and optically transparent. The basic structure of micro-emulsions is a swollen micellar solution. When water is the solvent, the systems are known as oil-in-water (O/W) micro-emulsions. Similarly, if the oil is the continuous phase and the water is within a reverse micelle, the system is water-in-oil (W/O) micro-emulsion. When the amounts of oil and water are nearly equal, a bicontinuous structure can be formed. These structures are the disordered analogues of the cubic and lamellar phases.

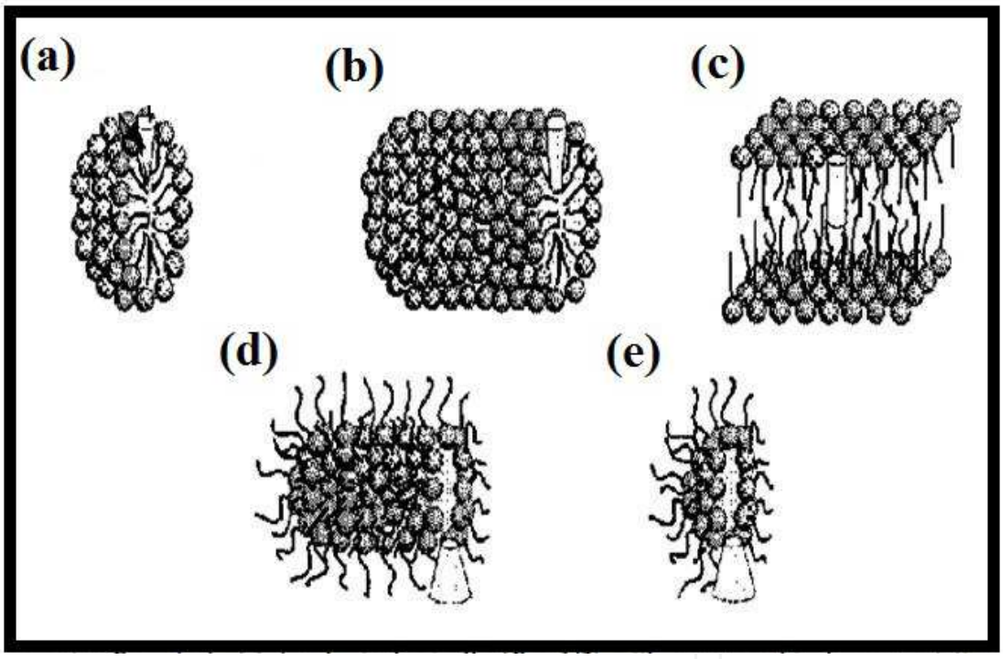

Fig. 3. Packing Parameter ($P=v/a_0l_c$). (a) Spherical Micelle ($P<1/3$) With a geographical Representation of the Three Values That Make up P. (b) A Cylindrical Micelle ($1/3<P<1/2$). (c) A Bilayer Sheet ($1/2<P<2$). (d) A Reverse Cylindrical Micelle ($2<P<3$). (e) A Reverse Spherical Micelle ($P>3$).

9. Polymers

Polymers are long chain-like giant molecules (macromolecules) made by the linkage of large numbers of small repeating molecules called monomers. Short chain lengths formed in the course of synthesis or degradation of polymers is called oligomers. The majority of

polymers, and the only ones considered here, are compounds of carbon. Polymers are very widespread and can be synthetic (e.g. nylon) or natural (e.g. rubber). They form vital components of living organisms, and the most important molecule, DNA, is a polymer of amino acids. Colloquially, polymers are often called plastics. More precisely, plastics are sometimes defined as polymers that can be easily formed at low temperatures, and sometimes as a pure polymer together with a nonpolymeric additive, which may be solid, liquid or gas. There are two main divisions of polymeric materials: thermoplastic and thermosetting. Thermoplastic materials can be formed repeatedly; that is, they can be melted and reformed a number of times. Thermosetting materials can be formed only once; they cannot be re-melted. They are usually strong, and are typified by resins. A further group of polymers merits mention, elastomers. Elastomers can be deformed a considerable amount and return to their original size rapidly when the force is removed. The properties of polymers depend both on the details of the carbon chain of the polymer molecule and on the way in which these chains fit together. The chain form can be linear, branched or cross linked, and a great variety of chemical groups can be linked to the chain backbone. The chains can be carefully packed to form crystals, or they can be tangled in amorphous regions. Amorphous polymers tend not to have a sharp melting point, but soften gradually. These materials are characterized by a glass transition temperature, Tg, and in a pure state are often transparent. Although polymers are associated with electrically insulating behavior, the increasing ability to control both the fabrication and the constitution of polymers has led to the development of polymers that show metallic conductivity superior to that of copper and to polymers that can conduct ions well enough to serve as polymer electrolytes in batteries and fuel cells.

9.1 History of conducting polymers

Historically, polymers have been considered as insulators and found application areas due to their insulating properties. Infact, so far, any electrical conduction in polymers which is generally due to loosely bound ions was mostly regarded as an undesirable fact. However, emerging as one of the most important materials in the twentieth century, the use of polymers move from primarily passive materials such as coatings and containers to active materials with useful optical, electronic, energy storage and mechanical properties. Indeed, discovery and study of conducting polymers have already started this development [Freund. M. S, 2006, Epstein. A. J, 1999 and Inzelt. G, 2008]. Electrically conducting polymers are defined as materials with an extended system of conjugated carbon-carbon double bonds (fig 4) [Advani. S. G, 2007]. They are synthesized either by reduction or oxidation reaction, which is called doping process, giving materials with electrical conductivities up to 105 S/cm. Conducting polymers are different from polymers filled with carbon black or metals, since the latter are only conductive if the individual conductive particles are mutually in contact and form a coherent phase.

Although conducting polymers are known as new materials in terms of their properties, the first work describing the synthesis of a conducting polymer was published in the ninetieth century. In 1862, Henry Letheby prepared polyaniline by anodic oxidation of aniline, which was conductive and showed electrochromic behavior. However, electronic properties of so called aniline black were not determined.

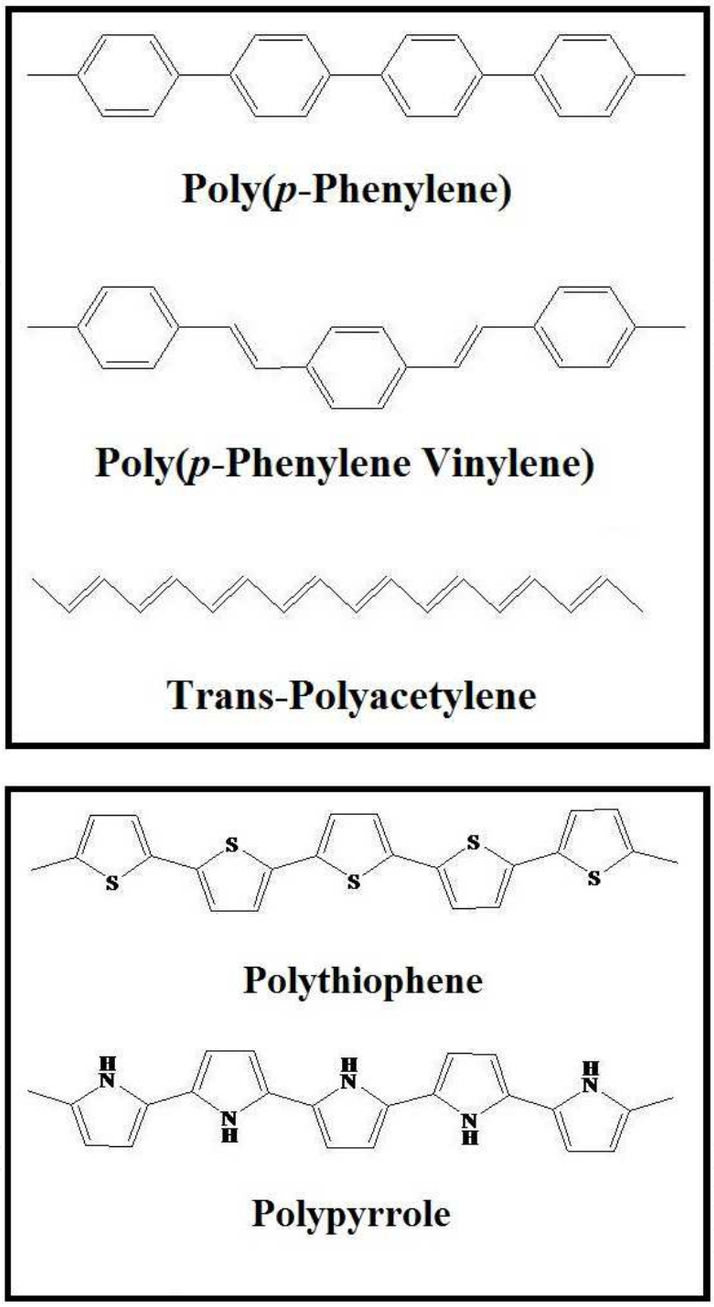

Fig. 4. Some Examples for Conducting Polymers.

In 1958, Natta et al. synthesized polyacetylene as a black powder which was found to be a semiconductor with conductivity in the range of 10-11 to 10-3 S/cm, depending on the process conditions of the polymer. In 1977, drawing attention on "conducting polymers", the first intrinsic electrically conducting organic polymer, doped polyacetylene, was reported. Intrinsically conducting polymers are a different class of materials than conducting polymers, which are a physical mixture of a non-conductive polymer with a conducting material such as metal or carbon powder. The preparation of polyacetylene by Sirakawa and coworkers and the

discovery of the large increase in its conductivity after "doping" by the group led by MacDiarmid and Heeger actually launched this new field of research.

Electronically conducting polymers possess a variety of properties related to their electrochemical behavior and are therefore active materials whose properties can be altered as a function of their electrochemical potential. The importance and potential impact of this new class of material was recognized by the world scientific community when Hideki Shirakawa, Alan J. Heeger and Alan G. MacDiarmid were awarded the Nobel Prize in Chemistry in 2000 "for the discovery and development of electronically conductive polymers".

9.2 Composites

A composite is defined as a material created by combination of two or more components namely, selected filler or reinforcing agent and a compatible matrix binder. The combination of these component results in formation of a new material with specific characteristics and properties. The synthetic assemblage of the components does not occur as a dissolvation but rather like merging into each other to act in concert. Although the components act together as a single material, both the components and the interface between them can usually be physically identified. Generally, the behavior and the properties of the composite are controlled by the interface of the components. Since the composite is a totally new material having new and specific characteristics, its properties cannot be achieved by any of its components acting alone.

The classification of composites can be done in different ways. The composites can be classified on the basis of the form of their structural components: (i) fibrous where the composite is composed of fibers in a matrix, (ii) laminar where the composite is composed of layers in a matrix, and (iii) particulate where the composite is composed of particles in a matrix [Kricheldorf. H. R, 2005, Lubin. G, 1982].

Another type of classification can be done on the basis of filler or reinforcing agent used namely polymer matrix composites (PMCs), metal matrix composites (MMCs), ceramic matrix composites (CMCs), carbon-carbon matrix composites (CCCs), intermetallic composites (IMCs), or hybrid composites [Sanjay. K, 2002].

9.3 Polymer matrix composites

Composite materials have been utilized to solve technological problems for a long time. In 1960s with the introduction of polymeric-based composites, composites start capturing the attention of industries. Since then, composite materials have become common engineering materials. They are designed and manufactured for various applications including automotive components, sporting goods, aerospace parts, consumer goods, and in the marine and oil industries. Increasing awareness of product performance and competition in the global market for lightweight components also supported the growth in composite usage. Among all materials, composite materials have the potential to replace widely used steel and aluminum, and many times with better performance. Replacing steel components with composite components can save 60 to 80% in component weight, and 20 to 50% weight by replacing aluminum parts. Today, it appears that composites are the materials of choice for many engineering applications.

The matrix material used in polymer-based composites can either be thermoset (epoxies, phenolics) or thermoplastic resins (low density polyethylene, high density polyethylene, polypropylene, nylon, acrylics). The filler or reinforcing agent can be chosen according to the desired properties. The properties of polymer matrix composites are determined by properties, orientation and concentration of fibers and properties of matrix.

The matrix has various functions such as providing rigidity, shaping the structure by transferring the load to fiber, isolating the fiber to stop or slow the propagation of crack, providing protection to reinforcing fibers against chemical attack and mechanical damage (wear), and affecting the performance characteristics such as ductility, impact strength, etc. depending on its type. The failure mode is strongly affected by the type of matrix material used in the composite as well as its compatibility with the fiber. The important functions of fibers include carrying the load, providing stiffness, strength, thermal stability, and other structural properties in the composites and providing electrical conductivity or insulation, depending on the type of fiber used [Omastova. M, 1998].

Polypropylene (PP) is one of the fastest growing commercial thermoplastics due to its attractive combination of low density and high heat distortion temperature. There are some limitations in physicochemical properties that restrict PP applications. A typical illustration is in packaging, where PP has poor oxygen gas barrier resistance. No single polymer has shown the ideal combination of performance features. PP possesses good water vapor barrier properties, but it is easily permeated by oxygen, carbon dioxide, and hydrocarbons. The necessity of developing more effective barrier polymers has given rise to different strategies to incorporate and optimize the features from several components. Most schemes to improve PP gas barrier properties involve either addition of higher barrier plastics via a multilayer structure (co-extrusion) or by introducing filler with high aspect ratio in the polymer matrix. 1. Co-extrusion allows tailoring of film properties through the use of different materials where each material component maintains its own set of properties, compared with blending of polymers in a mono-extrusion technique. Co-extrusion is used to generate multilayer laminate structures from separately extruded polymer films that are sandwiched together [109 and 110]. Resulting films may comprise many layers, such as the PP-adhesivepoly (ethylene-co-vinyl-alcohol) (EVOH)-adhesive PP system: EVOH barrier sheet trapped between two layers of moisture resistant PP and two additional adhesive strata. However, by nature co-extrusion is a complex and expensive process.

9.4 Composites of polypyrrole

Maria Omastova and Ivan Chodak prepared conductive polypropylene/polypyrrole composites using the method of chemically initiated oxidative modification of polypropylene particles in suspension by pyrrole. In order to prepare the composite, polypropylene particles were dispersed in water-methanol mixture and $FeCl_3$ was added to be used for chemical oxidation. Addition of pyrrole started formation of polypyrrole particles in polypropylene suspension. The electrical and rheological properties of the composite were compared with polypropylene/polypyrrole composite prepared by melt mixing of pure polypropylene with chemically synthesized polypyrrole and with polypropylene/carbon black composites also prepared by melt mixing. Elemental analysis verified presence of polypyrrole in polypropylene matrix. The conductivity studies show that even a very small PPy amount present in composites results in a significant increase in

conductivity. Processing conditions are observed to have a great effect on electrical conductivities of composites. The composite prepared by sintering PP particles covered with PPy shows about 7 orders of magnitude higher conductivity than the composite prepared by melt mixing of pure polypropylene with chemically synthesized polypyrrole whereas the conductivity of sintered PP/PPy composites is comparable to that of PP/Carbon black composite. The PP/CB and injection molded PP/PPy composites exhibit similar flow properties. However, for compresion molded PP/PPy composites a considerable increase of complex viscosity was observed [Pionteck. J, 1999].

10. Nanocomposites

Nanomaterials and nanocomposites have always existed in nature and have been used for centuries. However, it is only recently that characterization and control of structure at nanoscale have drawn intense interest for research and these materials start to represent new and exciting fields in material science. A nanocomposite is defined as a composite material where at least one of the dimensions of one of its constituents is on the nanometer size scale. In other words, nanocomposites can be considered as solid structures with nanometer-scale dimensional repeat distances between the different phases that constitute the structure. These materials typically consist of an inorganic (host) solid containing and an organic component or vice versa. They can consist of two or more inorganic/organic phases in some combinational form that at least one of the phases or features is in the nanosize.

In general, nanocomposite materials can exhibit different mechanical, electrical, optical, electrochemical, catalytic, and structural properties than those of each individual component. The multifunctional behavior for any specific property of the material is often more than the sum of the individual components [Mravcakova. M, 2006, Omoto. M, 1995, Ajayan. P. M, 2003 and Lee. E. S, 2004].

10.1 Polymer-based and polymer-filled nanocomposites

In recent years, the limits of optimizing composite properties of traditional micrometer-scale composite fillers have been reached due to the compromises of the obtained properties. Stiffness is traded for toughness, or toughness is obtained at the cost of optical clarity. In addition, regions of high or low volume fraction of filler often results in macroscopic defects which lead to breakdown or failure of the material. Recently, a new research area has provided the opportunity to overcome the limitations of traditional micrometer-scale polymer composites. This new investigation area is the nanoscale filled polymer composites where the filler is <100 nm in at least one dimension.

Implementation of the novel properties of nanocomposites strongly depends on processing methods that lead to controlled particle size distribution, dispersion, and interfacial interactions. Processing technologies for nanocomposites are different from those for composites with micrometer-scale fillers, and new developments in nanocomposite processing are among the reasons for their recent success.

Nanoscale fillers can be in many shapes and sizes, namely tube, plate-like or 3D particles. Fiber or tube fillers have a diameter <100 nm and an aspect ratio of at least 100. The aspect ratios can be as high as 106 (carbon nanotubes). Plate-like nanofillers are layered materials

typically with a thickness on the order of 1 nm, but with an aspect ratio in the other two dimensions of at least 25. Three dimensional (3D) nanofillers are relatively equi-axed particles <100 nm in their largest dimension. This is a convenient way to discuss polymer nanocomposites, because the processing methods used and the properties achieved depend strongly on the geometry of the fillers.

10.2 Nanocomposites of polypyrrole

Eun Seong Lee and Jae Hyung Park prepared in situ formed procesable polypyrrole nanoparticle/amphiphilic elastomer composites which could have applications in biosenors, semiconductors, artificial muscles, polymeric batteries and electrostatic dissipation due to their process ability and considerable conductivities. The polymerization process of pyrrole was achieved by chemical oxidation of the pyrrole monomer by $FeCl_3.6H_2O$ in the presence of multiblock copolymer dissolved in methanol/water mixture. The multiblock copolymer was used as a stabilizer during polypyrrole synthesis and when cast after removing the dissolved polymers, served as a flexible and elastomeric matrix. The polymerization time, concentration of multiblock copolymer and the oxidant, reaction medium composition were optimized in terms of conductivity measurements and the highest conductivity was reported as 3.0±0.2 Scm^{-1}. Mechanical properties such as tensile strength and elongation at break of the composites were found to increase with increasing amount of multiblock copolymer [Wu. T. M, 2008].

Tzong-Ming Wu and Shiang-Jie Yen have reported synthesis, characterization and properties of monodispersed magnetic coated multi-walled carbon nanotube/polypyrrole nanocomposites. Fe_3O_4 was used for coating multi-walled carbon nanotube (MWCNT). Fe_3O_4 coated c-MWCNT/PPy nanocomposites were synthesized via the in situ polymerization. The polymerization of pyrrole molecules was achieved on the surfaces of Fe_3O_4 coated c-MWCNT. The comparison of conductivities have shown that Fe_3O_4 coaed c-MWCNT/PPy nanocomposites have about 4 times higher conductivity that that of pure PPy matrix. Fe_3O_4 coated c- MWCNT/PPy nanocomposites were observed to exhibit ferromagnetic behaviour [Boukerma. K, 2006].

Kada Boukerma and Jean-Yves Piquemal prepared montmorillonite/polypyrrole nanocomposites and investigated their interfacial properties. The synthesis of MMT/PPy nanocomposites was achieved by in situ polymerization of pyrrole in the presence of MMT. Scanning electron microscopy results have shown that the surface morphology of the nanocomposites were more like the surface of untreated MMT. X-ray photoelectron spectroscopy (XPS) exhibited that the nanocomposites have MMT-rich surfaces which inicates intercalation of polypyrrole in the host galleries. The increase in interlamellar spacing was measured by transmission electron microscope. Invers gas chromatography measurements showed high surface energy of the nanocomposites [Mravcakova. M, 2006].

Miroslava Mravcakova and Kada Boukerma prepared montmorillonite/polypyrrole nanocomposites. The effects of organic modification of clay on the chemical and electrical properties were studied. The morphology investigations showed that the surface of MMT/PPy has a MMT-rich surface and relatively low conductivity (3.1×10^{-2} Scm^{-1}) indicating intercalation of PPy in the clay galleries. Whereas, the organically modified MMT/PPy nanocomposites have PPy-rich surface and higher conductivity indicating PPy

formation on the surface of MMT. The dispersive contribution of surface energy of o-MMT was measured to be significantly low compared to that of MMT due to the stearly chains from the ammonium chlorides used for organic modification [Ranaweera. A. U, 2007].

A.U. Ranaweera and H.M.N Bandara prepared electronically conducting montmorillonite-Cu_2S and montmorillonite-Cu_2S-polypyrrole nanocomposites. MMT-Cu_2S nanocomposite was prepared by cation-exchange approach and its conductivity was measured as 3.03×10^{-4} Sm^{-1}. The polymerization of pyrrole was achieved between the layers of MMT-Cu_2S to obtain MMT-Cu_2S-PPy nanocomposite. The characterization was performed by XRD, FT-IR and impedance measurements. The electronic conductivity was reported as 2.65 Sm^{-1} [Dallas. P, 2007].

Panagiotis Dallas and Dimitrios Niarchos reported interfacial polymerization of pyrrole and in situ synthesis of polypyrrole/silver nanocomposites. The oxidizing agents used were Ag(I) or Fe(III). Depending on using different surfactants (SDS or DTAB) or not using any surfactant, the average diameter of polypyrrole structures was observed to be in the range of 200-300 nm. The electron microscopy images exhibited different morphologies of polypyrrole depending on using various surfactants or not using any as well as the size and shape of the silver nanocomposites. X-ray diffractometry showed amorphous structure of polymers. Further characterization was performed by thermogravinetric analysis and FT-IR spectroscopy [Carotenuto. G, 1996].

10.3 Nanoparticle/polymer composite processing

There are three general ways of dispersing nanofillers in polymers. The first is direct mixing of the polymer and the nanoparticles either as discrete phases or in solution. The second is in-situ polymerization in the presence of the nanoparticles, and the third is both in-situ formation of the nanoparticles and in-situ polymerization. Due to intimate mixing of the two phases, the latter can result in composites called hybrid nanocomposites [Lee. E. S, 2004].

10.4 Direct mixing

Direct mixing is a well-known and established polymer processing technique. When these traditional melt-mixing or elastomeric mixing methods are feasible, they are the fastest method for introducing new products to market. Although melt mixing has been successful in many cases, for some polymers, due to rapid viscosity increase with the addition of significant volume fractions of nanofiller, this processing method has limitations. There are many examples showing melt mixing method for composite production and exhibiting some limitations for the process [Lee. E. S, 2004].

10.5 Solution mixing

In solution mixing, in order to overcome the limitations of melt mixing method, both the polymer and the nanoparticles are dissolved or dispersed in solution. This method enables modification of the particle surface without drying, which reduces particle agglomeration. After dissolvation the nanoparticle/polymer solution can be cast into a solid, or solvent evaporation or precipitation methods can be used for isolation of nanoparticle/polymer composite. Conventional techniques can be used for further processing [Lee. E. S, 2004].

10.6 In-situ polymerization

In in-situ polymerization, nanoscale particles are dispersed in the monomer or monomer solution, and the resulting mixture is polymerized by standard polymerization methods. This method provides the opportunity to graft the polymer onto the particle surface. Many different types of nanocomposites have been processed by in-situ polymerization. Some examples for in-situ polymerization are polypyrrole nanoparticle/amphiphilic elastomer composites; magnetite coated multi-walled carbon nanotube/polypyrrole nanocomposites and polypyrrole/ silver nanocomposites. The key to in-situ polymerization is appropriate dispersion of the filler in the monomer. This often requires modification of the particle surface because, although dispersion is easier in a liquid than in a viscous melt, the settling process is also more rapid.

11. Polypyrrole

Among the conjugated polymers, polypyrrole (PPy) is the most representative one for its easy polymerization and wide application in gas sensors, electrochromic devices and batteries. Polypyrrole can be produced in the form of powders, coatings, or films. It is intrinsically conductive, stable and can be quite easily produced also continuously. The preparation of polypyrrole by oxidation of pyrrole dates back to 1888 and by electrochemical polymerization to 1957. However, this organic p-system attracted general interest and was found to be electrically conductive in 1963. Polypyrrole has a high mechanical and chemical stability and can be produced continuously as flexible film (thickness 80 mm; trade name: Lutamer, BASF) by electrochemical techniques. Conductive polypyrrole films are obtained directly by anodic polymerization of pyrrole in aqueous or organic electrolytes.

Apart from electrochemical routes, polypyrrole can also be synthesized by simple chemical ways to obtain powders. Basically chemical oxidative polymerization methods can be used to synthesize bulk quantities of polypyrrole in a fast and easy way. Like other conducting polymers polypyrrole exhibit more limited environmental, thermal and chemical stability than conventional inert polymer due to the presence of dopant and its dynamic and electro active nature.

11.1 Synthesis of polypyrrole

Polypyrrole and many of its derivatives can be synthesized via simple chemical or electrochemical methods [120]. Photochemically initiated and enzyme-catalyzed polymerization routes have also been described but less developed. Different synthesis routes produce polypyrrole with different forms; chemical oxidations generally produce powders, while electrochemical synthesis leads to films deposited on the working electrode and enzymatic polymerization gives aqueous dispersions [Liu. Y. C, 2002, Tadros. T. H, 2005 and Wallace. G. G, 2003]. As mentioned above the electrochemical polymerization method is utilized extensively for production of electro active/conductive films. The film properties can be easily controlled by simply varying the electrolysis conditions such as electrode potential, current density, solvent, and electrolyte. It also enables control of thickness of the polymers. Electrochemical synthesis of polymers is a complex process and various factors such as the nature and concentration of monomer/electrolyte, cell conditions, the solvent, electrode, applied potential and temperature, pH affects the yield and the quality of the film.

Thus, optimization of all of the parameters in one experiment is difficult. In contrast, chemical polymerization does not require any special instruments; it is a rather simple and fast process. Chemical polymerization method involves oxidative polymerization of pyrrole monomer by chemical oxidants either in aqueous or non-aqueous solvents or oxidation by chemical vapor deposition in order to produce bulk polypyrrole as fine powders. Fe(III) chloride and water are found to be the best oxidant and solvent for chemical polymerization of pyrrole respectively regarding desirable conductivity characteristics.

Previous studies have shown that the optimum initial mole ratio of Fe(III)/Pyrrole for polymerization by aqueous Fe(III) chloride solution at 19 ˚C is 2.25 or 2.33. Also, several studies have revealed that factor such as solvent, reaction temperature, time, nature and concentration of oxidizing agent; affect the oxidation potential of the solution which affects the final conductivity of the product.

S.Goel and A. Gupta synthesized polypyrrole samples of different nanodimensions and morphologies by time dependent interfacial polymerization reaction. Pure chloroform was used as solvent for pyrrole and ammonium persulphate dissolved in HCl was used as the oxidizing solution. The polymerization occurred in the interface of organic and aqueous phases and polypyrrole was formed as thin layer on the interface. Morphology study of polypyrrole nanoparticles was done by scanning electron microscopy and transmission electron microscopy.

Yang Liu and Ying Chu synthesized polypyrrole nanoparticles through microemulsion polymerization. Alcohol-assisted microemulsion polymerization was performed in order to adjust the inner structure of polypyrrole nanoparticles for polymerization SDS was used as the surfactant, water was used as the solvent and aqueous solution of $NH_4S_2O_8$ was used as the oxidant. Characterization of polpyrrole was done by FT-IR and morphology study was performed by SEM and TEM. Hongxia Wang and Tong Lin synthesized polypyrrole nanoparticles by oxidation of pyrrole with ferric chloride solution during microemulsion polymerization process. Dodecyltrimethyl ammonium bromide (DTAB) was used as the surfactant. Particle characaterisation was performed by using FTIR, elemental analysis, UV-VIS spectra and SEM. Variation of particle size from about 50 to 100 and 100 to 200 nm with the change in surfactant concentration was reported. Xinyu Zhang and Sanjeev K. Manohar synthesized narrow pore-diameter polypyrrole nanotubes. The synthesis was performed by chemical oxidative polymerization of pyrrole using $FeCl_3$ oxidant and V_2O_5 nanofibers as the sacrificial template producing microns long electrically conducting polypyrrole nanotubes having 6 nm averages pore diameter. M.R. Karim and C.J. Lee synthesized polypyrrole by radiolysis polymerization method. Conducting PPy was synthesized by the in situ gamma radiation-induced chemical oxidative polymerization method. This method was reported to provide highly uniform polymer morphology. Jyongsik Jang and Joon H. Oh, synthesized polypyrrole nanoparticles via microemulsion polymerization with using various surfactants. Fe(III) chloride was used as the oxidant. The selective fabrication of amorphous polypyrrole nanoparticles as small as 2 nm in diameter using microemulsion polymerization at low temperature was reported.

12. Polypropylene

Polypropylene (PP) is a thermoplastic material that is produced by polymerization of propylene molecules into very long polymer molecule or chains (fig 5.). There are number of

different ways to link the monomers together, but its most widely used form is made with catalysts that produce crystallizable polymer chains. The resulting product is a semi crystalline solid with good physical, mechanical, and thermal properties. Another form of PP produced in much lower volumes as a byproduct of semi crystalline PP production and having very poor mechanical and thermal properties, is a soft, tacky material used in adhesives, sealants, and caulk products. The above two products are often referred to as "isotactic" (crystallizable) PP (i-PP) and "atactic" (noncrystallizable) PP (-PP), respectively.

The average length of the polymer chains and the breadth of distribution of the polymer chain lengths determine the main properties of PP. In the solid state, the main properties of the PP reflect the type and amount of crystalline and amorphous regions formed from the polymer chains. Polypropylene has excellent and desirable physical, mechanical and thermal properties when used in room temperature applications. It is relatively stiff and has a high melting point, low density and relatively good resistance to impact.

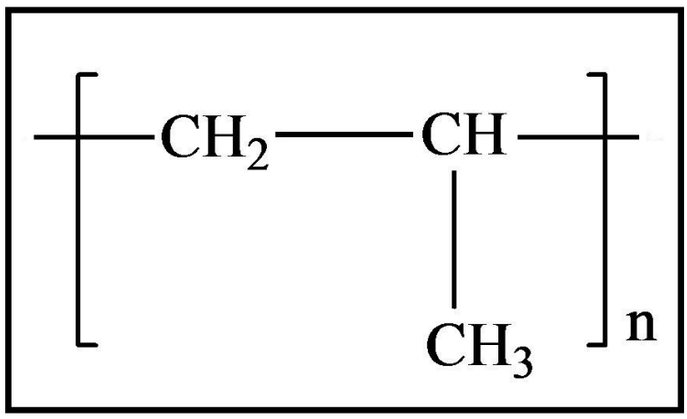

Fig. 5. Structural of Polypropylene.

Among conjugated polymers polypyrrole has attracted great interest due to its high conductivity, good thermal and environmental stability and ease of synthesis. However, it is an infusible, inprocessable Synthesis, characterization, and application of polyethylene glycol modified insulin polymer having relatively poor mechanical properties. On the other hand, polypropylene is a well-known insulating thermoplastic with outstanding mechanical properties. In this study, the synergistic assemblage of polypyrrole with polypropylene is investigated. Synthesis of polypyrrole nanoparticles via microemulsion polymerization, preparation of PP/PPy nanocomposites in order to provide some level of process ability to infusible and inprocessable PPy while inducing conductivity to insulating PP and preparation of PP/PPy nanocomposites with dispersant in order to improve the dispersion of PPy nanoparticles using identical procedures.

12.1 Preparation of PP/PPy nanocomposites

PP/PPy nanocomposites were prepared by melt mixing of pure PP with PPy using Brabender Plasti-Corder. The composition of nanocomposites varied between 1-20% PPy by weight. In order to provide a regular shape, the nanocomposites were pressed in a mould followed by fast cooling. The identical procedure is employed with addition of 2% by weight dispersant (SDS) during mixing process of pure PP with PPy.

12.2 Synthesis of polypyrrole nanoparticles

Synthesis of polypyrrole nanoparticles was achieved using micro-emulsion polymerization system by oxidation of pyrrole monomer with $FeCl_3.6H_2O$. As the oxidant was added, the color of the solution changed from colorless to deep greenish black which is an indication of oxidation of conducting polypyrrole. The reaction product polypyrrole was obtained in the form of black powder.

12.3 Scanning electron microscope analysis of polypyrrole nanoparticles

Scanning electron microscopy was performed in order to investigate the dimensions and the morphology of polypyrrole nanoparticles. The scanning electron micrographs of polypyrrole nanoparticles are presented in fig 6. The SEM micrographs of polypyrrole exhibited globular, nanometer-sized particles. The polypyrrole nanoparticles are observed

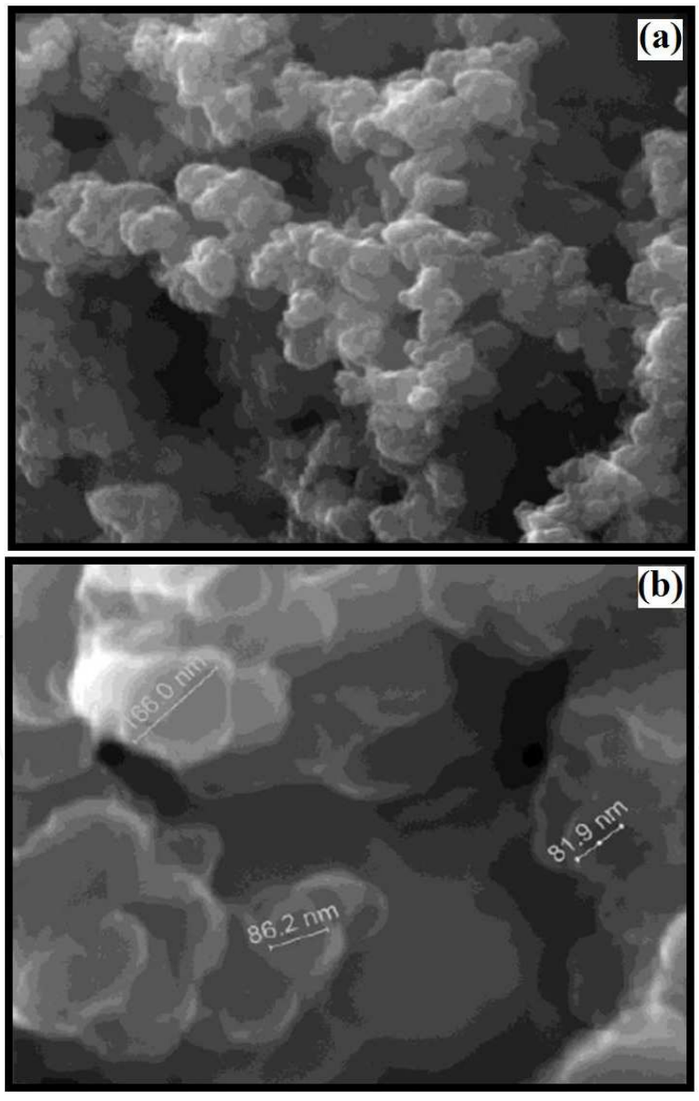

Fig. 6. SEM micrographs of PPy nanoparticles at magnifications of (a) 80000, (b) 300000.

to have a distribution of dimensions between 50 to 150 nm. The SEM results confirm that micro-emulsion polymerization system was successful in the synthesis of nano-sized polypyrrole particles. The SEM results prove that the micro-emulsion polymerization system provided similar dimensions of PPy nanoparticles with previous studies where 50 to 100 nm and 100 to 200 nm polypyrrole nanoparticles were reported.

12.4 Preparation of PP/PPy nanocomposites

The polypyrrole nanoparticles prepared by micro-emulsion polymerization system were mixed with polypropylene in order to provide some level of process ability to infusible and inprocessable polypyrrole while inducing conductivity to insulating polypropylene. In order to obtain PP/PPy nanocomposites, the polypyrrole nanoparticles were mixed with polypropylene by melt mixing technique followed by pressing to give a regular shape to nanocomposites. The nanocomposites were processed with injection molding and several black colored dog-bone shaped samples were obtained successfully. The composition of nanocomposites varied in the range of 1 to 20% by weight polypyrrole nanoparticles in polypropylene.

12.5 Characterization of PP/PPy nanocomposites

Mechanical properties of PP/PPy nanocomposites were investigated by tensile tests. The effect of loading different amounts of polypyrrole nanoparticles into thermoplastic polypropylene matrix and the changes in mechanical properties produced by incorporation of polypyrrole nanoparticles were examined. In order to understand the effect of using sodium dodecylsulphate as dispersant in PP/PPy nanocomposites, identical tests were performed also for the nanocomposites prepared with dispersant.

A stress-strain curve is known to provide information about both linear elastic properties and mechanical properties related to plastic deformation of a material. In order to specify a material as ductile or brittle, the response of the material to applied stress is investigated. The area under stress-strain curve corresponds to the energy required to break the material. As it is clearly seen in fig 7. pure PP is very ductile at a test rate of 5 cm/min and the area under the curve is very large indicating the great energy required to break the material. The Young's modulus, tensile strength and percentage strain at break values of pure polypropylene are 430 MPa, 27.8 MPa and %424 respectively.

The changes in mechanical properties that are produced by loading different amounts of polypyrrole nanoparticles can be well understood from stress-strain curves of PP/PPy nanocomposites which are illustrated in fig 8. through 3.8. As it is clearly observed in stress-strain curves of nanocomposites, addition of polypyrrole nanoparticles makes polypropylene matrix very brittle. In fact, addition of even the smallest amount of polypyrrole which is 1% causes a dramatic decrease in the energy required to break it.

The changes in mechanical properties that are produced by loading different amounts of polypyrrole nanoparticles can be well understood from stress-strain curves of PP/PPy nanocomposites which are illustrated in fig 8. through 3.8. As it is clearly observed in stress-strain curves of nanocomposites, addition of polypyrrole nanoparticles makes

polypropylene matrix very brittle. In fact, addition of even the smallest amount of polypyrrole which is 1% causes a dramatic decrease in the energy required to break it.

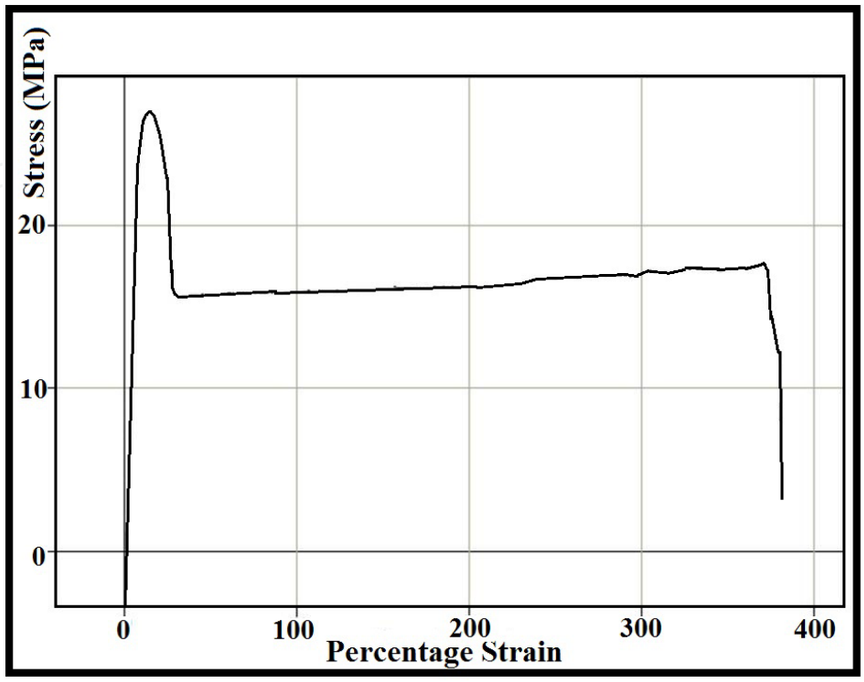

Fig. 7. Stress vs strain curve of pure PP.

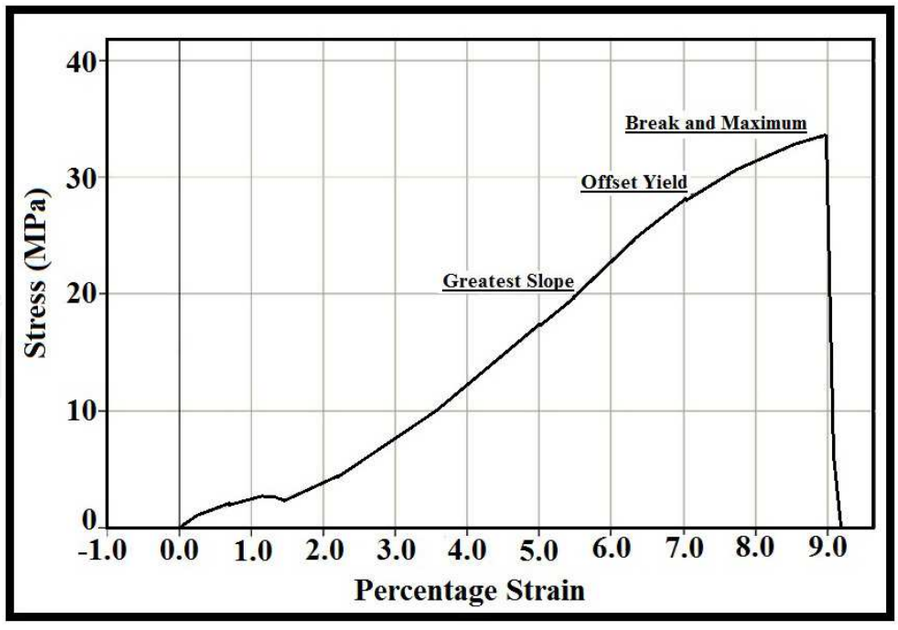

Fig. 8. Stress vs strain curve for PP/1%PPy nanocomposite without dispersant.

PPy nanoparticles in PP enhanced the strength and the stiffness of the nanocomposites. The greatest change for both properties was observed in PP/1%PPy nanocomposite. As it is seen

in fig 9. and fig 10. incorporation of 1% PPy into PP matrix increased the tensile strength and Young's modulus of pure PP considerably. Increasing amount of PPy nanoparticles in PP matrix caused gradual increase in both tensile strength and Young's modulus of nanocomposites until addition of 10% PPy nanoparticles. Further addition of PPy nanoparticles slightly changes the tensile strength and Young's modulus.

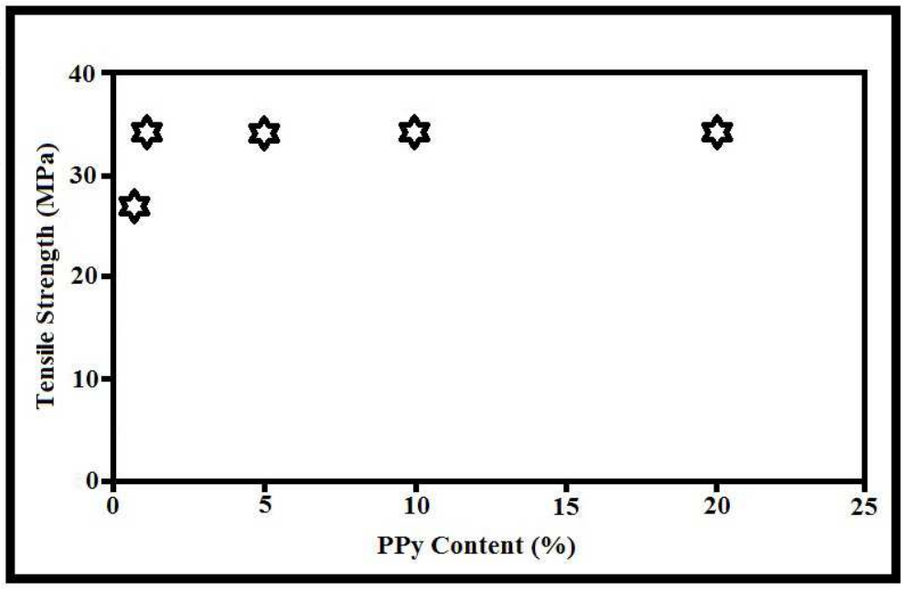

Fig. 9. Tensile strength vs PPy content for PP/PPy nanocomposites without dispersant.

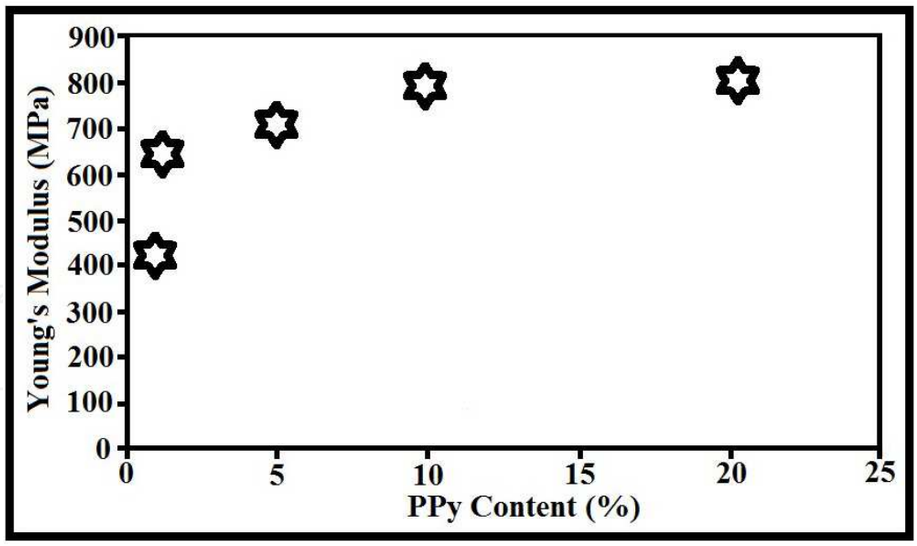

Fig. 10. Young's Modulus vs PPy Content For PP/PPy Nanocomposites Without Dispersant.

The tensile test results of PP/PPy nanocomposites show that incorporation of PPy nanoparticles in PP improves the strength and the stiffness while limiting the elongation of PP. In order to investigate the potential improvement in dispersion of PPy nanoparticles in PP, identical tensile tests were employed to nanocomposites prepared with dispersant. Due

to the effect of dispersant, the interaction between PPy nanoparticles with PP matrix is expected to be improved. The Young's modulus, tensile strength and percentage strain at break values for nanocomposites prepared with dispersant are presented in Table. 1.

PPy Content (w%)	Young's Modulus (MPa)	Tensile Strength (MPa)	Percentage Strain at Break (%)
0	430±10	27.8±0.5	424±9.0
1	583±77	30.1±0.4	14.4±0.2
5	748±53	32.8±0.6	9.3±0.9
10	786±10	32.9±0.4	8.0±0.3
20	831±31	33.2±0.6	7.1±0.2

Table 1. Young's Modulus, Tensile Strength, Percentage Strain Values For PP, PP/PPy Nanocomposites With 2% Dispersant by Weight.

The change in percentage strain at break, Young's modulus and tensile strength with increasing polypyrrole content in nanocomposites prepared with dispersant are shown in fig 11. through fig 13. The gradual decrease in percentage strain at break values for increasing amounts of PPy is clearly seen in fig 11. Addition of 1% PPy caused a significant decrease in percentage strain since it prevents extension of PP matrix.

However, the decrease in percentage strain is relatively smaller due to binding effect of dispersant used. fig 12 and fig 13 exhibit the increase in tensile strength and Young's modulus of the nanocompoites with addition of PPy.

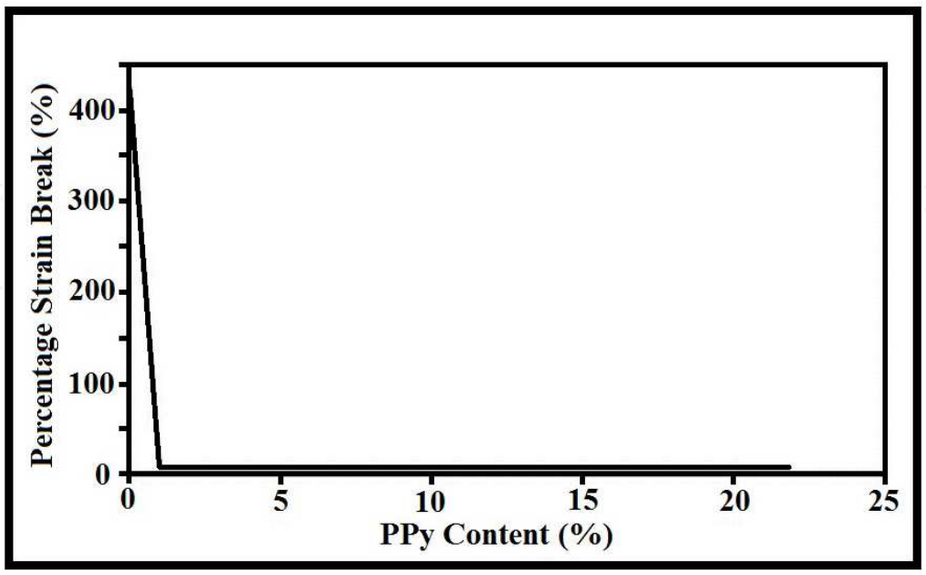

Fig. 11. Percentage strain at break vs PPy content for PP/PPy nanocomposites with dispersant.

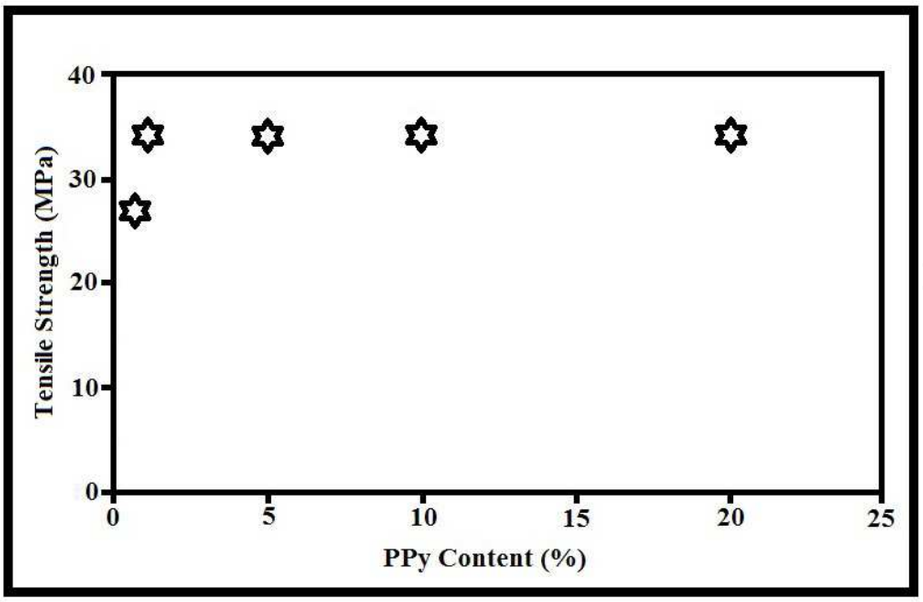

Fig. 12. Tensile strength vs PPy content for PP/PPy nanocomposites with dispersant.

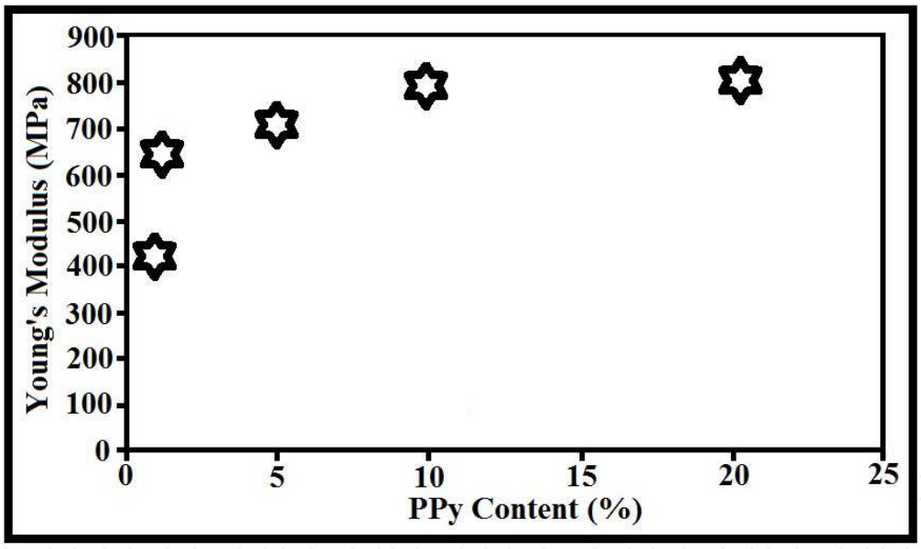

Fig. 13. Young's modulus vs PPy content for PP/PPy nanocomposites with dispersant.

The increase in both tensile strength and Young's modulus with increasing PPy content indicates the reinforcing action of PPy. In order to investigate the potential effect of dispersant in enhancement of dispersion of PPy nanoparticles, the change in tensile strength and percentage strain at break and Young's modulus for both nanocomposite sets prepared without and with dispersant are examined (Table. 1.).

The obtained results show that addition of PPy nanoparticles leads to a similar increase in tensile strength and Young's modulus of pure PP in both nanocomposite sets. Although the values are not identical, the values for nanocomposites involving dispersant did not exhibit significant difference compared to ones prepared without dispersant. However, the effect of

dispersant is perceived in percentage strain at break values. The nanocomposites prepared using dispersant exhibited a regular decrease in percentage strain at break while a sudden decrease was observed for nanocomposites prepared without dispersant. The percentage strain at break values for PP/1%PPy nanocomposite prepared with and without dispersant are found to be 15.3 and 9.5 respectively. The higher decrease in nanocomposite prepared without dispersant can be explained by considering weaker interaction of polypyrrole with polypropylene. Same case is true for also nanocomposites with 5% polypyrrole content. Although, similar behavior was observed for nanocomposites with 10% and 20% polypyrrole content, the difference in values are not as considerable as the ones for nanocomposites with 1% and 5% PPy content.

13. Application of polypropylene derivatives in synthesis of nanomaterials

13.1 Metaloxide nanoparticles

Nanoparticles of MO (NP-CuO) were prepared by a novel sonochemistry route from metal acetate and sodium hydroxide in the presence of polypropylene derivatives such as polyethylene glycol, polypropylene glycol and polyvinyl alcohol. Variations in several parameters and their effects on the structural properties of nanoparticles (particle size and morphology) were investigated. 0.05 M solution of metal acetate in the presence of polyethylene glycol gave the best results. The characterizations were carried out by X-Ray diffraction, scanning electron microscopy, IR spectroscopy, thermal gravimetric analysis and differential thermal analysis.

Ultrasonic irradiation and stabilizer (PPG, PEG and PVA) can greatly enhance the conversion rate of precursor to nanometer- sized MO particles in the presence of polyethylene glycol (PEG), polypropylene glycol (PPG) and polyvinyl alcohol (PVA). Also the role of calcinations, time, and concentration of metal acetate solution and power of ultrasound wave on the size, morphology and chemical composition of nanoparticles was investigated. For the precursor, we used metal acetate dissolved in ethanol/water/(PEG or PPG or PVA). Then MO nanoparticles were directly obtained by addition of a solution of sodium hydroxide. The influence of several parameters on the size and morphology of MO particles was reported. The powders were characterized by powder X-Ray Diffraction (XRD), Scanning Electron Microscopy (SEM), IR spectroscopy, Thermal Gravimetric Analysis and Differential Thermal Analysis (TGA/DTA).

13.2 CuO nanoparticles

Different amounts of NaOH solution with a concentration of 0.1 M were added to the 0.1, 0.05, 0.025 M solutions of Cu acetate in ethanol/water. The obtained mixtures were sonicated for 30-60 min with different ultrasound powers. To investigate the role of surfactants on the size and morphology of nanoparticles, we used 0.5g of polypropylene derivatives in the reactions with optimized conditions. Table 1 shows the conditions of reactions in detail. A multiwave ultrasonic generator (Bandlin Sonopuls Gerate-Typ: UW 3200, Germany) equipped with a converter/transducer and titanium oscillator (horn), 12.5 mm in diameter, operating at 30 kHz with a maximum power output of 780 W, was used for the ultrasonic irradiation. The ultrasonic generator automatically adjusted the power level. The wave amplitude in each experiment was adjusted as needed. The X-ray powder

diffraction (XRD) measurements were performed using a Philips diffractometer of X′pert Company with mono chromatized Cuk_{α} radiation. The crystallite sizes of the selected samples were estimated using the Scherrer method. TGA and DTA curves were recorded using a PL-STA 1500 device manufactured by Thermal Sciences. The samples were then characterized using a scanning electron microscope (SEM) (Philips XL 30) with gold coating.

Sample	$Cu(OAc)_2.2H_2O$	NaOH (0.1 M)	Aging time	Ultrasound power	Template
1	50 ml (0.1 M)	100 ml	1 hr	30W	PEG
2	50 ml (0.05 M)	100 ml	1 hr	30W	PEG
3	50 ml (0.025 M)	100 ml	1 hr	30W	PEG
4	50 ml (0.1 M)	100 ml	1 hr	45W	PEG
5	50 ml (0.05 M)	100 ml	1 hr	45W	PEG
6	50 ml (0.025 M)	100 ml	1 hr	45W	PEG
7	50 ml (0.1 M)	100 ml	30 min	30W	PEG
8	50 ml (0.05 M)	100 ml	30 min	30W	PEG
9	50 ml (0.025 M)	100 ml	30 min	30W	PEG
10	50 ml (0.1 M)	100 ml	30 min	45W	PEG
11	50 ml (0.05 M)	100 ml	30 min	45W	PEG
12	50 ml (0.025 M)	100 ml	30 min	45W	PEG
13	50 ml (0.1 M)	100 ml	1 hr	30W	PPG
14	50 ml (0.05 M)	100 ml	1 hr	30W	PPG
15	50 ml (0.025 M)	100 ml	1 hr	30W	PPG
16	50 ml (0.1 M)	100 ml	1 hr	45W	PPG
17	50 ml (0.05 M)	100 ml	1 hr	45W	PPG
18	50 ml (0.025 M)	100 ml	1 hr	45W	PPG
19	50 ml (0.1 M)	100 ml	30 min	30W	PPG
20	50 ml (0.05 M)	100 ml	30 min	30W	PPG
21	50 ml (0.025 M)	100 ml	30 min	30W	PPG
22	50 ml (0.1 M)	100 ml	30 min	45W	PPG
23	50 ml (0.05 M)	100 ml	30 min	45W	PPG
24	50 ml (0.025 M)	100 ml	30 min	45W	PPG
25	50 ml (0.1 M)	100 ml	1 hr	30W	PVA
26	50 ml (0.05 M)	100 ml	1 hr	30W	PVA
27	50 ml (0.025 M)	100 ml	1 hr	30W	PVA
28	50 ml (0.1 M)	100 ml	1 hr	45W	PVA
29	50 ml (0.05 M)	100 ml	1 hr	45W	PVA
30	50 ml (0.025 M)	100 ml	1 hr	45W	PVA
31	50 ml (0.1 M)	200 ml	30 min	30W	PVA
2	50 ml (0.05 M)	200 ml	30 min	30W	PVA
33	50 ml (0.025 M)	100 ml	30 min	30W	PVA
34	50 ml (0.1 M)	100 ml	30 min	45W	PVA
35	50 ml (0.05 M)	100 ml	30 min	45W	PVA
36	50 ml (0.025 M)	100 ml	30 min	45W	PVA

Table 2. Experimental Conditions For Preparation of CuO Nanoparticles.

Fig 14a. shows the XRD patterns of CuO nanoparticles. fig 1shows the XRD pattern of the direct sonochemicaly synthesized CuO nanoparticles and fig (14b, 14c and 14d) show the XRD patterns of this sample after calcinations for 2 hours at 500 °C. Sharp diffraction peaks shown in fig 14 indicates good crystallinity of CuO nanoparticles. No characteristic peak related to any impurity was observed. The broadening of the peaks indicates that the particles were of nanometer scale. The average size of the particles of the some samples (the best result from 36 reactions) was 80 nm, and the average size of these samples after calcinations at 500 °C for 2 hours were calculated as about 70 nm. These findings are in agreement with those observed from the SEM images.

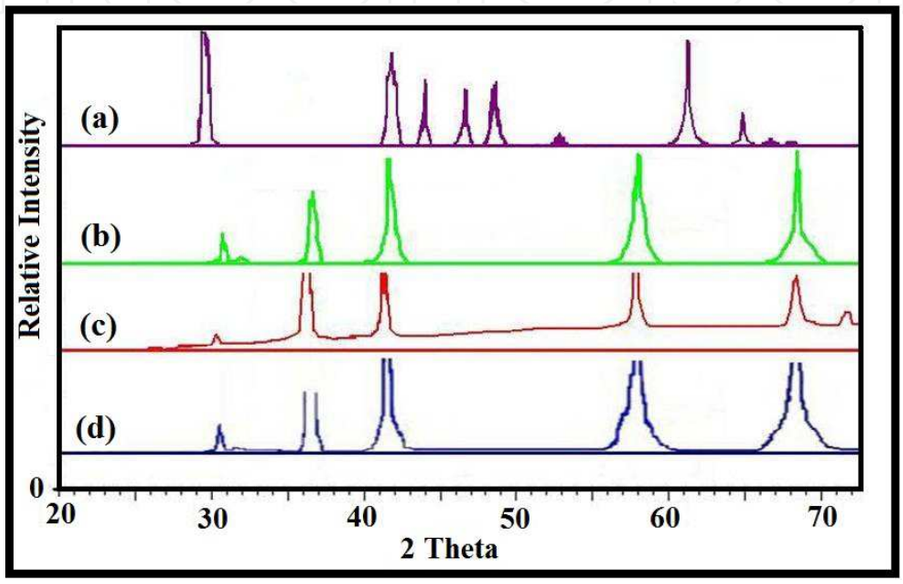

Fig. 14. X-Ray Powder Diffraction Pattern of CuO Nanoparticles (Sample No. 2) (a) Before Calcinations, (b) After Calcination (PEG Template), (c) After Calcination (PVA Template) and (d) After Calcinations (PPG Template).

The morphology, structure and size of the samples were investigated by Scanning Electron Microscopy (SEM). fig 15a indicates that the original morphology of the particles was approximately spherical with the diameter varying between 35 to 103 nm. The best morphology with smaller particles and good distribution was obtained for the sample number 2 before calcinations. fig 15b shows the SEM images of these samples after calcinations with different concentrations, it is clear from the fig 15b that the size of the particles has become small after calcinations. fig 15c shows the SEM images of the sample number 10. The role of PEG on the morphology of this sample is obvious. It has been reported that the presence of a capping molecule (such as polyvinyl alcohol, polyethylene glycol and polypropylene glycol) can alter the surface energy of crystallographic surfaces in order to promote the anisotropic growth of the nanoparticles. PEG is adsorbed on the crystal nuclei and helps the particles to grow separately. To investigate the size distribution of the nanoparticles, a particle size histogram was prepared for the sample No 2, (fig 16). Most of the particles possess sizes in the range from 30 to 103 nm. For further demonstration.

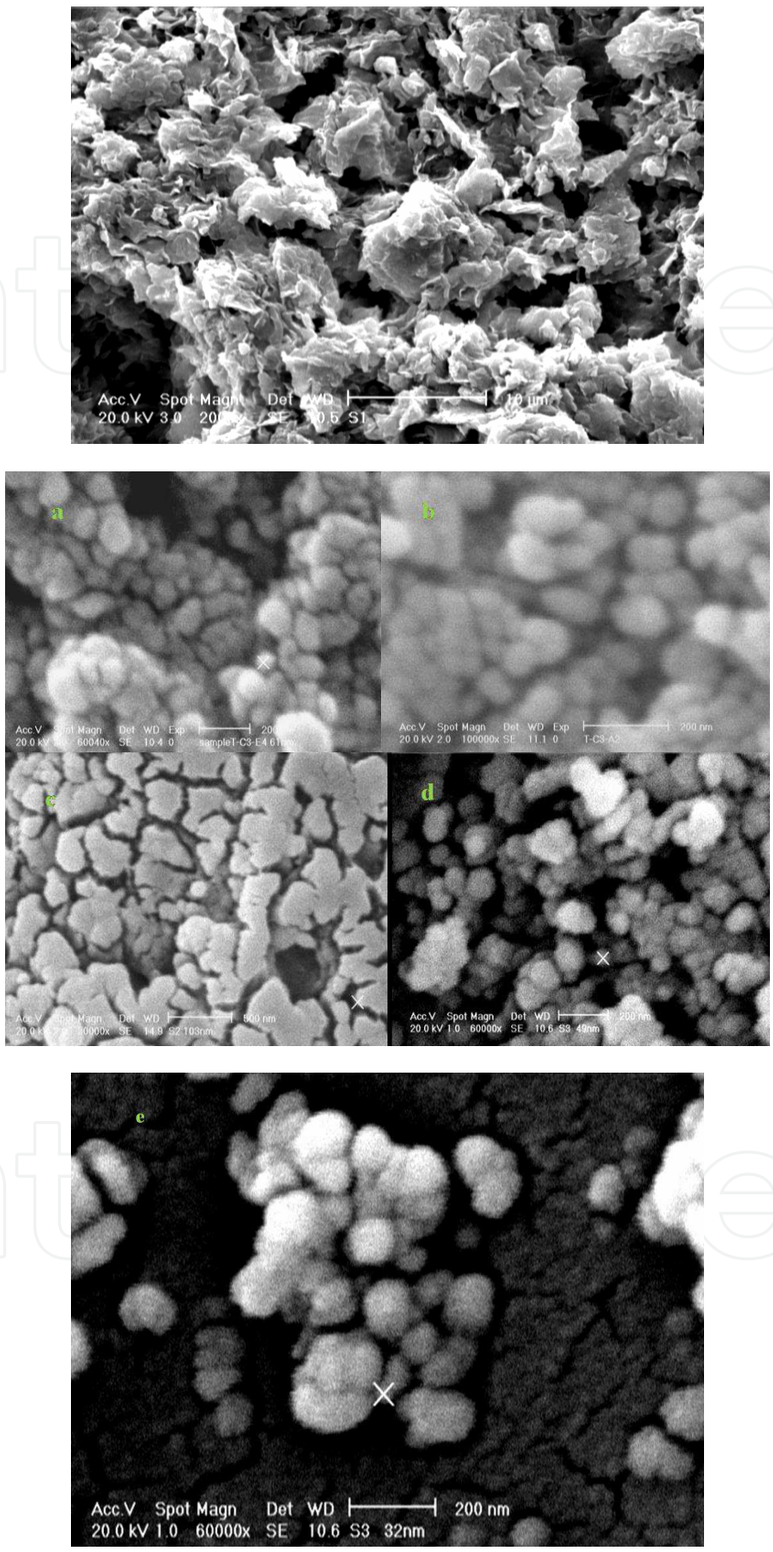

Fig. 15. The SEM images of CuO nanoparticles; (a) sample No. 2 before calcination, (b) samples No. 1(a), 3(b), 4(c), 5(d) after calcination, (c) sample No. 2 after calcinations.

Thermo-gravimetric analyses (TGA) were carried out to show that there was no difference between the curves of intermediate products and the one after calcinations. The results showed that there was no notable loss of weight in the TGA curves, proving the existence of CuO, which does not decompose at this temperature range. Further, the similarity of the TG curves of two samples shows the direct synthesis of CuO. fig 17a shows the TGA diagrams of the sample No. 2, and copper acetate and the compound before calcinations. fig 17b shows the DTA diagrams of the sample No. 2, copper acetate and the compound before calcinations.

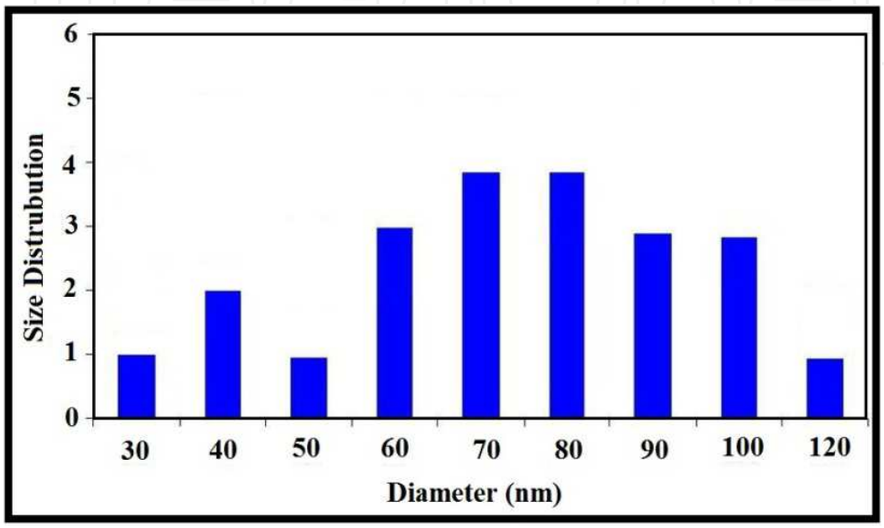

Fig. 16. Particle size histogram for the sample 2.

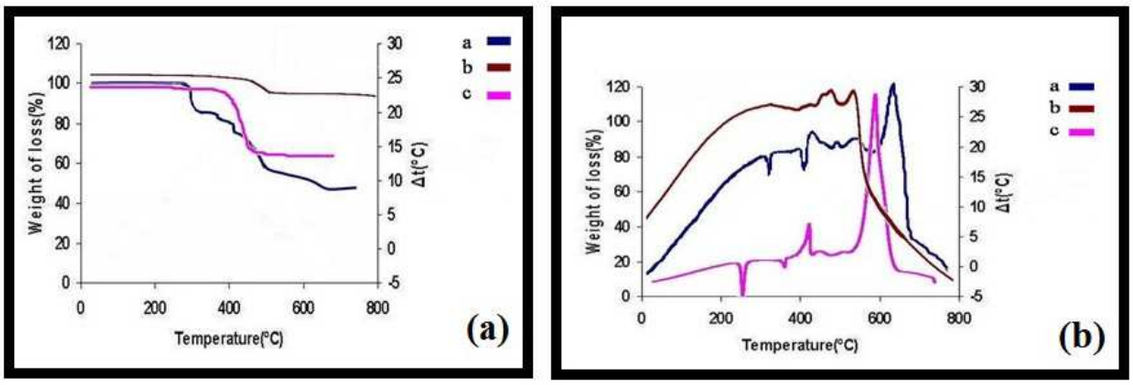

Fig. 17. The TG- DTA curves of CuO nanoparticles of the sample No. 2.

In order to investigate the role of sonication on the composition, size and morphology of the products, we carried out the reaction without sonication with the same conditions of the optimized sample. The XRD patterns of the obtained product corresponds to CuO but the SEM images show that the nanoparticles of the samples without using sonication have larger sizes as compared with the samples obtained via the sonochemical route.

It was indicated that the NP-CuO could decompose the organic pollutants by formation of exceed super oxides and/or hydroxyl radicals at the CuO interface.

13.3 Other M(II) oxide nanoparticles

Some nano-sized metal oxid (MO) such as ZnO, NiO and MnO were successfully synthesized by sonochemistry method in solutions at room temperature. The reactants used are ($M(Ac)_2.2H_2O$) and sodium hydroxide (NaOH), and H_2O/EtOH as a carrier in polyethylene glycol (PEG) template. Some of parameters such as effect concentration of NaOH solution, ultrasound power and sonicating time in growth and morphology of the nano-structures were investigated. The best morphology with smaller particles size and good distribution was obtained by using 0.025 M solution of NaOH and 45 w ultrasound powers in 1 h sonicating time. The particle size of the nano-sized metal oxid powders synthesized at room temperature is approximately between 40–80 nm. The resulting nano-sized powder was characterized by X-ray diffraction (XRD) measurements, Raman, BET, Solid state UV-vis and Scanning Electron Microscopy (SEM).

In recent years, metal oxide (MO) nanoparticles as a kind of functional material has attracted extensive interests due to its novel optical, electronic, magnetic, thermal and mechanical properties and potential application in catalyst, battery electrodes, gas sensors, electrochemical films, photo-electronic devices, and so on. In these applications, it is still needed for synthesizing high-quality and ultra-fine powders with required characteristics in terms of their size, morphology, microstructure, composition purity, crystallizability, etc. which are the most essential factors which eventually determine the microstructure and performance of the final products. Therefore, it is very important to control the powder properties during the preparation process. There are many chemical and physical methods to prepare nanometer MO, including the precipitation of metal acetate with NaOH. Recently, the interest preparation of nanometer MO has been growing. However, only few practical methods have been reported. The nanomaterials whose synthesis was reported are ZnS, Sb_2S_3, HgSe, SnS_2, CdS, CdSe, PbX (E = S, Se, Te, O), CuS, Ag_2Se and $CdCO_3$. But the sonochemical method for preparation of nanomaterials is very interesting, simple, cheap and safe. However, we have developed a simple sonochemical method to prepare NiO, MnO and ZnO nanostructures, wherein MO is synthesized by the reaction of $(CH_3CO_2)_2M.2H_2O$ and NaOH in an ultrasonic device. The MO nanoparticles have been characterized by X-ray powder diffraction (XRD), Raman spectroscopy, Solid state UV, BET and also the morphology and size of the nanostructures have been observed by scanning electron microscopy (SEM). We have performed these reactions in several conditions to find out the role of different factors such as the aging time of the reaction in the ultrasonic device and the concentration of the metal acetate on the morphology of nanostructures.

Typical procedure for preparation of MO nanoparticles: NaOH solution with a concentration of 0.1 M (100 ml) were added to the 0.05 and 0.025 M solutions of $M(CH_3COO)_2.2H_2O$ in ethanol/water. To investigate the role of surfactants on the size and morphology of nanoparticles, we used 0.5 gr of polyethylene glycol (PEG) in the reaction with optimized conditions. The mixtures were sonicated for 30-60 min, with different ultrasound powers followed by centrifuging with a centrifuge, and separation of the solid and liquid phases. The solid phase was washed for three times ethanol and water. Finally, the washed solid phase was calcinated at 500 ^oC for 30 min. Table 1 shows the conditions of reactions in detail. A multiwave ultrasonic generator (Bandlin Sonopuls Gerate-Typ: UW 3200, Germany) equipped with a converter/transducer and titanium oscillator (horn), 12.5 mm in diameter, operating at 30 kHz with a maximum power output of 780W, was used for

the ultrasonic irradiation. The ultrasonic generator automatically adjusted the power level. The wave amplitude in each experiment was adjusted as needed. X-ray powder diffraction (XRD) measurements were performed using a Philips diffractometer of X'pert Company with mono chromatized Cuk_{α} radiation. The samples were characterized with a scanning electron microscope (SEM) (Philips XL 30) with gold coating. Raman spectra were recorded on a Labram HR 800-Jobin Yvon Horbiba spectrometer. UVeVis spectra were measured with an HP 8453 diode array spectrophotometer. The specific surface area of samples was determined using the Brunauer–Emmet–Teller (BET) method in a volumetric adsorption apparatus (ASAP 2010 M, Micrometritics Instrument Corp).

Various conditions for preparation of MO nano-structures were summarized in Table. 3.

Series 1	$Mn(OAc)_2.2H_2O$	NaOH (0.1 M)	Aging time	Ultrasound power	Template
1	50 ml (0.05 M)	100 ml	1 hr	30W	PEG
2	50 ml (0.05 M)	100 ml	1 hr	45W	PEG
3	50 ml (0.025 M)	100 ml	1 hr	30W	PEG
4	50 ml (0.025 M)	100 ml	1 hr	45W	PEG
5	50 ml (0.05 M)	100 ml	30 min	30W	PEG
6	50 ml (0.05 M)	100 ml	30 min	45W	PEG
7	50 ml (0.025 M)	100 ml	30 min	30W	PEG
8	50 ml (0.025 M)	100 ml	30 min	45W	PEG
Series 2	$Ni(OAc)_2.2H_2O$	NaOH (0.1 M)	Aging time	Ultrasound power	Template
1	50 ml (0.05 M)	100 ml	1 hr	30W	PEG
2	50 ml (0.05 M)	100 ml	1 hr	45W	PEG
3	50 ml (0.025 M)	100 ml	1 hr	30W	PEG
4	50 ml (0.025 M)	100 ml	1 hr	45W	PEG
5	50 ml (0.05 M)	100 ml	30 min	30W	PEG
6	50 ml (0.05 M)	100 ml	30 min	45W	PEG
7	50 ml (0.025 M)	100 ml	30 min	30W	PEG
8	50 ml (0.025 M)	100 ml	30 min	45W	PEG
Series 3	$Zn(OAc)_2.2H_2O$	NaOH (0.1 M)	Aging time	Ultrasound power	Template
1	50 ml (0.05 M)	100 ml	1 hr	30W	PEG
2	50 ml (0.05 M)	100 ml	1 hr	45W	PEG
3	50 ml (0.025 M)	100 ml	1 hr	30W	PEG
4	50 ml (0.025 M)	100 ml	1 hr	45W	PEG
5	50 ml (0.05 M)	100 ml	30 min	30W	PEG
6	50 ml (0.05 M)	100 ml	30 min	45W	PEG
7	50 ml (0.025 M)	100 ml	30 min	30W	PEG
8	50 ml (0.025 M)	100 ml	30 min	45W	PEG

Table 3. Experimental conditions for the preparation of MO nanoparticles

The best morphology with smaller particles and good distribution was obtained for the sample number 4 in series 1, 2 and 3. fig 18(a,b and c) shows the XRD patterns of the direct sonochemicaly synthesized of the ZnO, NiO and MnO nanoparticles respectively. Sharp diffraction peaks shown in fig 18. indicate good crystallinity of MO nanoparticles. No characteristic peak related to any impurity was observed.

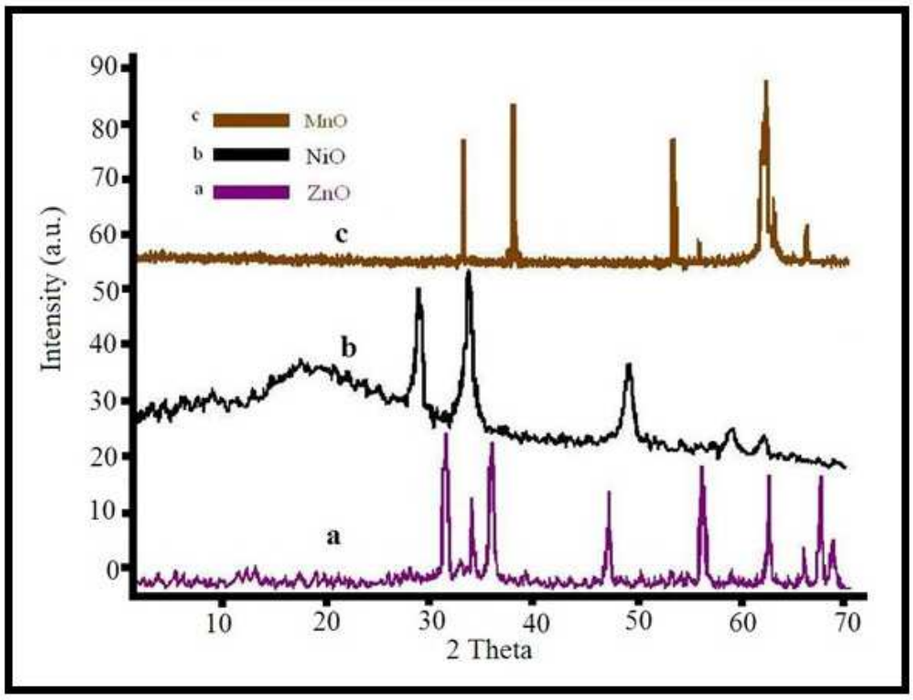

Fig. 18. X- Ray powder diffraction pattern of MO nanoparticles (a) ZnO, (b) NiO, (c) MnO.

The broadening of the peaks indicated that the particles were of nanometer scale. The morphology, structure and size of the samples are investigated by Scanning Electron Microscopy (SEM). fig 19 indicates that the original morphology of the ZnO, NiO and MnO particles are approximately spherical with the diameter varying between 40 to 80 nm. The role of PEG on the morphology of this sample is obvious. It has been reported that the presence of a capping molecule such as polyethylene glycol (PEG) can alter the surface energy of crystallographic surfaces, in order to promote the anisotropic growth of the nano particles. In this work PEG adsorbs on the crystal nuclei and it helps the particles to grow separately. To investigate the size distribution of the nano particles, a particle size histogram was prepared for MO nano particles, (fig 20).

Fig 21. demonstrates the UV-vis spectrum of the MO nanoparticles by ultrasonically dispersing in absolute ethanol. Strong absorption peak in the UV region can be observed. The absorption band gap *Eg* is usually achieved with the aid of the following equation:

$$(\alpha h\nu)^n = B(h\nu - E_g)$$

Concretely, $h\nu$ is the photo energy; a is the absorption coefficient; B is the constant related to the material; and n indicates either 2 or 1/2 for direct transition and indirect transition, respectively.

The inset of fig 21 gives us the typical $(ah\nu)^2 \sim h\nu$ curve for the MO samples calcinated at 500 °C. By the extrapolation of *Eg.* (1), we can get the present band gaps as 4.1, 3.7 and 3.9 Ev (layout for NiO, ZnO and MnO) indicating the small blue shifts upon size reductions for MO nanoparticles.

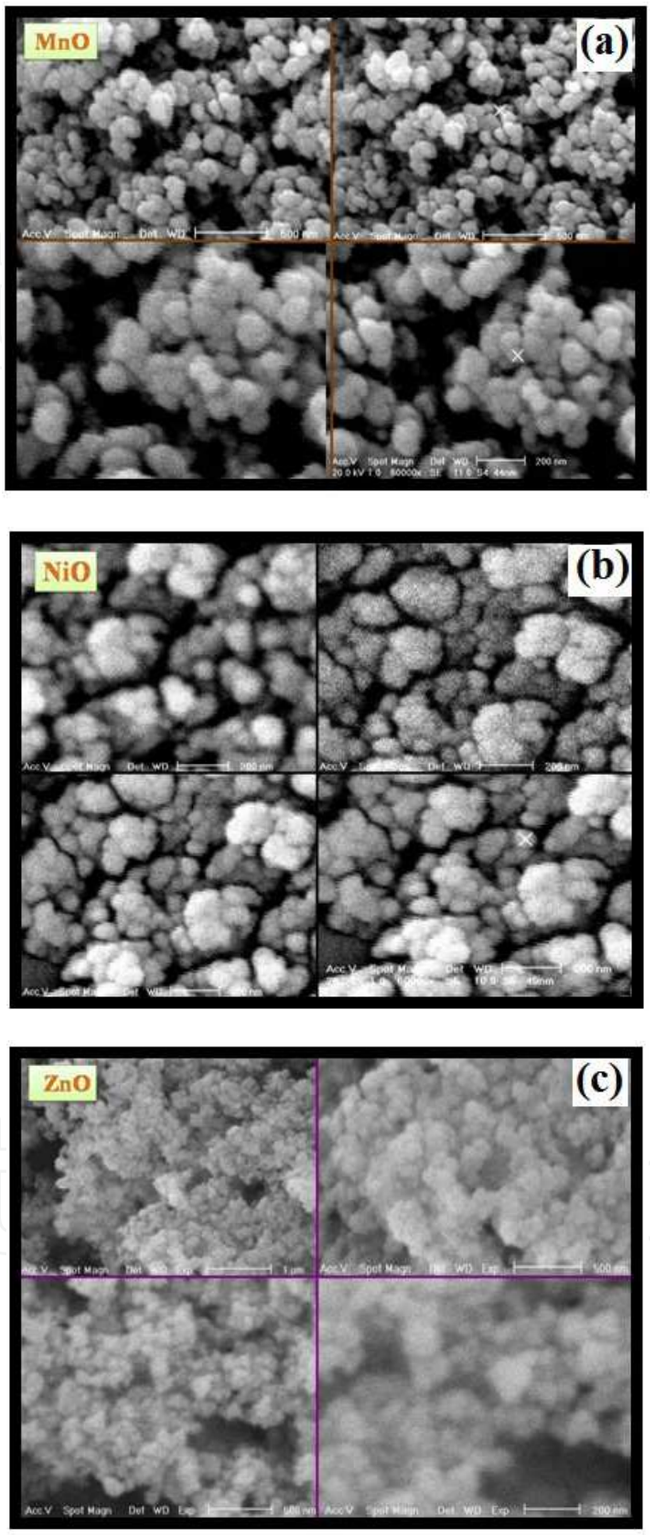

Fig. 19. Typical SEM micrographs of MO nano particles after calcinations: (a) ZnO, (b) NiO and (c) MnO.

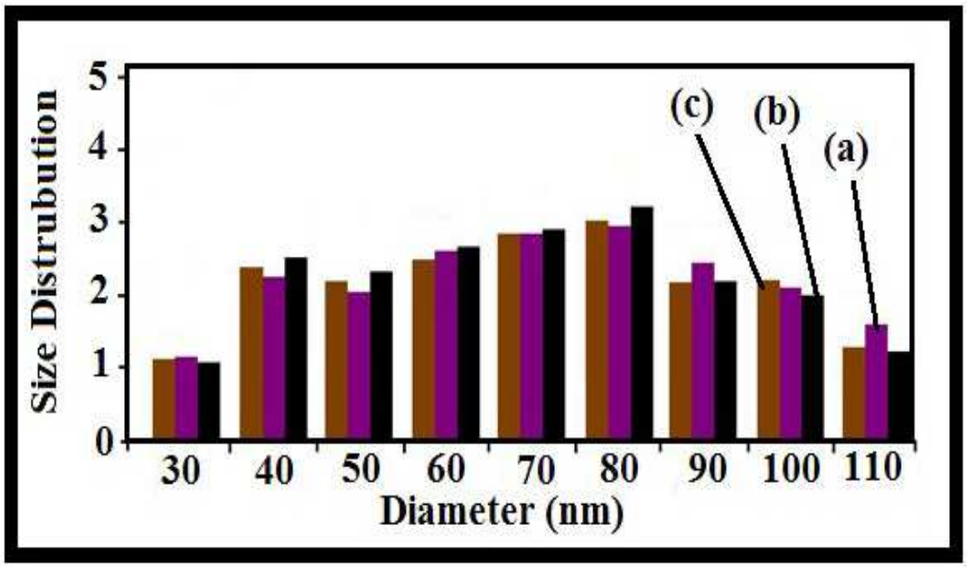

Fig. 20. Particle size Histogram of MnO, NiO and ZnO Nanopowders.

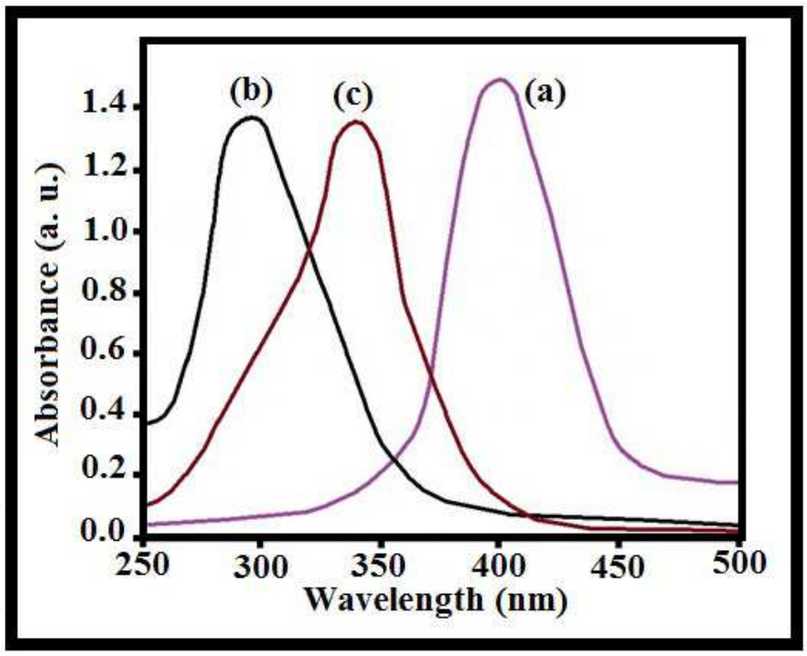

Fig. 21. Solid state UV absorption of MnO, NiO and ZnO nanoparticles

The surface area analysis was carried out on MO nanoparticles by BET method. Assuming the particles possess solid, spherical shape with smooth surface and same size, the surface area can be related to the average equivalent particle size by the equation:

$$D_{BET} = 6000/(\rho\, Sw) \text{ (in nm)}$$

Where D_{BET} is the average diameter of a spherical particle; *Sw* represents the measured surface area of the powder in m^2/g; and ρ is the theoretical density in g/cm^3. fig 22 shows

BET plots of MO nanoparticles, the specific surface area of MO nanoparticles calculated using the multi-point BET-equation are 33, 40 and 53 m^2/g (layout for NiO, ZnO and MnO), and the calculated average equivalent particle size is 36, 42 and 51 nm (layout for NiO, ZnO and MnO). We noticed that the particles size obtained from the BET and the SEM methods, agree very well with the result given by X-ray line broadening. The results of SEM observations and BET methods further confirmed and verified the relevant results obtained by XRD as mentioned above. Metal oxides are important catalyst in organic chemistry, gas sensors (such as CO_2, NO, SO_2, H_2O and CO) and battery cathode in the course of our research. The results of this investigation will be reported soon.

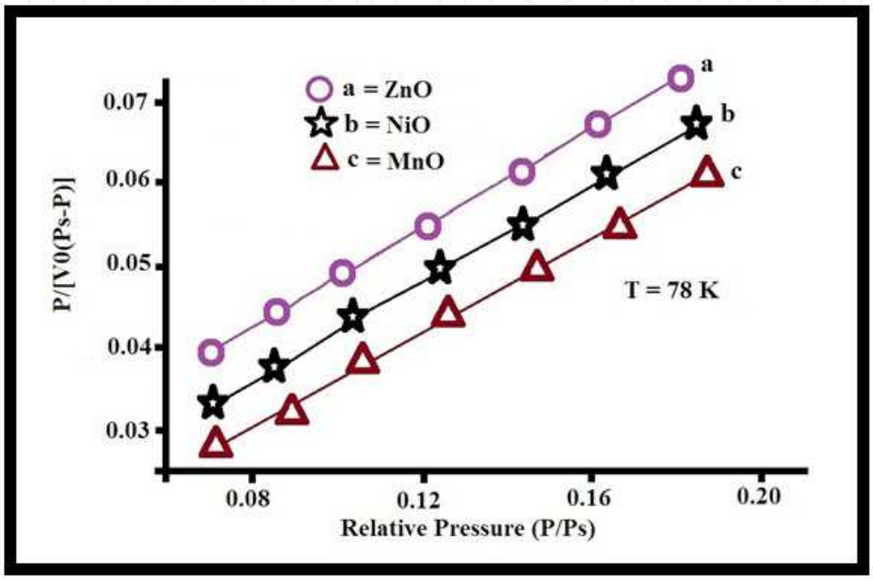

Fig. 22. BET plots of MnO, NiO and ZnO nanoparticles

Therefore Nano-sized of MnO, NiO and ZnO (MO) have been prepared by reaction between corresponding metal acetate and NaOH under ultrasound irradiation in solution at room temperature. Some of parameters such as effect concentration of NaOH solution, ultrasound power and sonicating time in growth and morphology of the nano-structures were investigated. The best morphology with smaller particles size and good distribution was obtained by using 0.025 M solution of metal acetate and 45 w ultrasound powers in 1 h sonicating time. Average particle sizes of the synthesized nano-sized MO powders were between 40-80 nm. Simple procedure, short reaction times, yields smaller particles and mild reaction conditions at room temperature are noteworthy advantages of this method. The specific surface area of MO nanoparticles calculated using the multi-point BET-equation are 33, 40 and 53 m^2/g (layout for NiO, ZnO and MnO), and the calculated average equivalent particle size is 36, 42 and 51 nm (layout for NiO, ZnO and MnO). We noticed that the particles size obtained from the BET and the SEM methods, agree very well with the result given by X-ray line broadening. The results of SEM observations and BET methods further confirmed and verified the relevant results obtained by XRD as mentioned above. The infrared absorption band of the MO nanoparticles show blue-shifts compared with that of bulk MO [Alireza Aslani, 2008[a], 2009[b], 2010[c] and 2011[d]].

14. References

A. Duteil, R. Q U. M. Chaudret, C. Roucauj,. S. Bradley, Chem. Mater. 1993. 5: 341.
Advani. S. G, Processing and Properties of Nanocomposites, World Scientific, pp. 1, 2007.
Ajayan. P. M, Schadler, L.S., Braun, P.V., Nanocomposite Science and Technology, Wiley, VCH pp 10, 77-80, 111, 112, 2003.
Alireza Aslani and A. Morsali. Inorganica Chimica Acta. 362, (2009), 5012-5016.
Alireza Aslani and V. Oroojpour. Physica B, Physics of Condensed matter. 406, (2011), 144-149.
Alireza Aslani, A. Morsali and M. Zeller. Solid State Sciences, 10, (2008), 1591-1597.
Alireza Aslani, A. Morsali, V. T. Yilmaz and C. Kazak. 929, (2009), 187-192.
Alireza Aslani, A. R. B. Shamili and K. Kaviani. Physica B, Physics of Condensed matter, 405, (2010), 3972–3976.
Alireza Aslani, A. R. B. Shamili and S. Barzegar. Physica B, Physics of Condensed matter, 405 (2010), 3585–3589.
Alireza Aslani, M. R. Arefi, A. Babapoor, A. Amiri, K. B. Shuraki. Applied Surface Science, 257, (2011), 4885-4889.
Alireza Aslani, Physica B, Physics of Condensed matter. 406, (2011), 150-154.
Alireza Aslani, V. Oroojpour, M. Fallahi, Applied Surface Science, 257, (2011), 4056-4061.
Bhandarkar, S, and A. Bose, J. Colloid Interface Sci., Vol. 135, No. 2, 1990, pp. 541–550.
Bliznyuk. V. N, A. Campbell, and C. W. Frank, ACS Symposium Series 695, New York Oxford University Press, 1998, pp. 220–232.
Bonnell. D. A, New York: Wiley-VCH, 2001.
Boukerma. K, Piquemal. J. Y, Chehimi. M. M, Mravcakova. M, Omastova. M, Beaunier. P, Polymer, 47, pp 569-576, 2006.
Brust, M, et al., J. Chem. Soc. Chem. Comm., Vol. 7, 1994, pp. 801–802.
Carotenuto. G, Her.Y. S, Matijevic. E, Ind. Eng. Chem. Res., 35,2929, 1996.
Collier, C. P, et al., Science, Vol. 277, No. 5334, 1997, pp. 1978–1981.
Cortan, A. R, et al, J. Am. Chem. Soc., Vol. 112, No. 4, 1990, pp. 1327–1332.
Dallas. P, Niarchos. D, Vrbanic. D, Boukos. N, Pejovnik. S, Trapalis. C, Petridis. D, Polymer 48, pp 2007-2013, 2007.
Edelstein, A. S, and R. C. Cammarata, Bristol, PA: IoP Publishing, 1996.
Epstein. A. J, Platics Design Library, 1, 93, 1999.
F. Wakai, Y. K, S. S. N. M, K. I and K. N, Nature, 344, 6265, 421-423 (1990).
Freund. M. S, Deore B., Self-Doped Conducting Polymers, Wiley, pp.1,2, 10-12, 2006.
Gabriel. B. L, SEM, A User's Manual for Materials Science, American Society for Metals, 1985.
Greffet. J. J, and R. Carminati, Progr. Surf. Sci., Vol. 56, No. 3, 1997, pp. 133–237.
H. Hirai, Macromol. Chem. Suppl. 1985, 14, 55.
H. Hirai, Y. Nakao, N. Toshima, J. Macromol. Sci. Chem. 1979. 13, 727.
H. Maeda, J. Control. Release, 19, 315–324 (1992).
H. Suzuki, T. Ohno, J. Soc. Powder Technol, Jpn, 39, 877–884 (2002).
I. Matsui, J. Chem. Eng, Jpn, 38(8), 535–546 (2005).
Inzelt. G, Conducting Polymers A New Era in Electrochemistry, Springer, 1, 2008.
J. S. Bradley, in Clusters and Colloids, G. SCHMID (ed.) VCH, Weinheim, 1993, p. 459.
K. Ishikawa, J. Soc. Powder Technol, Jpn, 38, 731-740 (2001).
K. Ishikawa, K. Yoshikawa and N. Okada, Phys. Rev. B, 37, 5852-5855 (1988).

K. Kobayashi, J. Soc. Powder Technol, Jpn, 41, 473-478 (2004).
K. Megure, Y. Nakamura. Y. Hayashim, . Torizuka, K. Esumi, Bull. Chem. Soc.]pn. 1988. 61. 347.
K. Niihara, J. Ceram. Soc. Jpn, 99 (10), 974-982 (1991).
K. Uchino, E. Sadanaga and T. Hirose, J. Am. Ceram. Soc, 72(8), 1555–1558 (1989).
Keyse. R. J, et al. Microscopy Handbook, Vol. 39, Oxford, England: BIOS Scientific Publishers, 1998.
Kitaigorodski. A. L, Organic Chemical Christallography, New York: Counsultants Bureau, 1961.
Kricheldorf. H. R, Nuyken, O., Swift, G., Handbook of Polymer Synthesis, Marcel Dekker., Ch. 12, pp 1,3,4, USA, 2005.
Lee. E. S, Park. J. H., Wallace. G. G., Bae. Y. H, Polymer International, 53:400-405, 2004.
Li, S, et al., IEEE Trans. on Magnetics, Vol. 37, No. 4, 2001, pp. 2350–2352.
Liu. Y. C, Materials Chemistry and Physics 77, pp 791-795, 2002.
Lover, T, et al., Chem. Mater. Vol. 9, No. 4, 1997, pp. 967–975.
Lubin. G, Handbook of Composites, Van Nostrand Reinhold Company Inc., USA, pp1, 2, 1982.
Lvov, Y. M, M. R. Byre and D. Bloor, Crystall. Reports, Vol. 39, No. 4, 1994, pp. 696–716.
Lvov, Y. M., et al, Phil. Mag. Lett., Vol. 59, No. 6, 1989, pp. 317–323.
Lvov. Y, and H. Mohwald, (eds.), New York: Basel/Marcel Dekker, 2000, pp. 125–167.
Lvov. Y. M, and L. A. Feigin, Kristallografiya, Vol. 32, No. 3, 1987, pp. 800–815.
M. Arakawa, Funsai (The Micrometrics), No 27, 54–64 (1983).
M. Arakawa, J. Soc. Powder Technol, Jpn, 42, 582–585 (2005).
M. E. Labib, R. Williams, Colloid Interface Sci. 1984. 97, 356.
M. Haruta, Catalysts, 36(6) 310-318 (1994).
M. Komiyama, H. Hirai, Bull. Chem. Soc. Jpn. 1983, 56, 2833.
M. Takashige, T. Nakamura, Jpn. J. Appl. Phys, 20, 43-46 (1981).
Mann, S., et al., J. Chem. Soc.-Dalton Trans., No. 4, 1983, pp. 771–774.
Mann, S., J. P. Hannington, and R. J. P. Williams, Nature, Vol. 324, No. 6097, 1986, pp. 565–567.
Mravcakova. M, Boukerma. K, Omastova. M, Chehimi. M. M, Materials Science and Engineering C, 26, pp 306-313, 2006.
Mravcakova. M, Omastova. M, Potschke. P, Pozsgy. A, Pukanszky. B., Pionteck. J, Adv. Technol., 17: 715-726, 2006.
N. Wada, Chem. Eng., 9, 17–21 (1984).
Nabok. A. V, et al, IEEE Trans. on Nanotechnology, Vol. 2, No. 1, 2003, pp. 44-49.
Nabok.A. V, et al., Thin Solid Films, Vol. 327–329, 1998, pp. 510–514.
Nakanishi, T. B. Ohtani, and K. Uosaki, J. Phys. Chem. B, Vol. 102, No. 9, 1998, pp. 1571–1577.
Netzer, L., and J. Sagiv, J. Am. Chem. Soc., Vol. 105, No. 3, 1983, pp. 674–676.
Omastova. M, Chodak. I, Pionteck. J, Potschke. P, Journal of Macromolecular Science, Part A, 35:7, 1117-1126, 1998.
Omoto. M, Yamamoto. T, Kise. H, Journal of Applied Polymer Science, Vol. 55, 283-287, 1995.
P. H. Hess, P. H. Parker, Appl. Polymer. Sci 1966. 10, 1915.

Petty. M. C, in Languir- Blodgett Films, G. G. Roberts, (ed.), New York: Plenum Press, 1990, pp. 133–221.
Petty. M. C, M. R. Bryce, and D. Bloor, (eds.), New York: Oxford University Press, 1995.
Pionteck. J, Omastova. M, Potschke. P, Simon. F, Chodak. I, Journal of Macromolecular Science, Part B, 38:5, 737-748, 1999.
Puntes, V. F, and K. M Krishnan, IEEE Trans. on Magnetics, Vol. 37, No. 4, 2001, pp. 2210–2212.
R. R. Karimi, A. R. B. Shamili, Alireza Aslani and K. Kaviani. Physica B, Physics of Condensed matter, 405, (2010), 3096–3100.
Ranaweera. A. U, Bandara. H. M. N, Rajapakse. R. M. G, Electrochimica Acta, 52, pp 7203-7209, 2007.
Rizza, R, et al, Chem. Mater., Vol. 9. No. 12, 1997, pp. 2969–2982.
Roberts, G. G, Adv. Phys., Vol. 34. No. 4, 1985, pp. 475–512.
Roberts, G. G, in Langmuir-Blodgett Films, G. G. Roberts, (ed.), New York: Plenum Press, 1990.
Roberts, G. G., et al., J. Verwey, (ed.), North Holland: Amsterdam, 1983, p. 141.
Rogach, A. L, et al., J. Phys. Chem. B, Vol. 103, No. 16, 1999, pp. 3065–3069.
Ross, J, and G. G. Roberts, Proceedings of 2nd International Meeting on Chemical Sensors, Bordeaux, France, 1986, p. 704.
S. Sato, N. Asai and M. Yonese, Colloid Polym. Sci, 274, 889-893 (1996).
Sanjay. K. Mazumdar, CRC Press LLC, USA, pp 4-6, 2002.
Sarathy, K. V., et al, J. Phys. Chem. B., Vol. 103, No. 3, 1999, pp. 399–401.
Schultz, D. L., et al, IEEE, 25th PVSC, Washington, D.C., May 13–17, 1996, pp. 929–932.
Stefanis. A, and A. A. G. Tomlinson, Enfield, NH: Trans Tech. Publications, 2001.
T. Sekino, Mater. Integr, 13(11) 50-54 (2000).
T. Yokoyama, Sokeizai, 3, 6-11 (2005).
Tadros. T. H, Applied Surfactants, Wiley-VCH Verlag GmbH and Co. KGaA, pp. 1-5, 2005.
Talapin, D. V, et al., Physica E, Vol. 14, No. 1–2, 2002, pp. 237–241.
Tredgold. R. H, Order in Thin Organic Films, Cambridge, England: Cambridge University Press, 1994.
Tsukruk. V. V, Progr. Polym. Sci., Vol. 22, No. 2, 1997, pp. 247–311.
Ulman. A, (ed.), Boston, MA: Butterworth- Heinemann, 1995.
Ulman. A, From Langmuir-Blodgett to Self- Assembly, Boston, MA: Academic Press, 1991.
V. H. Thiele, J. Kowallik. J. Colloid Sci. 1965. 20, 679.
Vogel, W, et al, Vol. 16, No. 4, 2000, pp. 2032–2037.
Wallace. G. G, Spinks, G. M, Kane-Maguire. L. A. P, Teasdale. P. R, CRC Press LCC, USA, pp.51, 2003.
Wegner. G, Molecular Crystals and Liquid Crystals Science, Vol. 234, 1993, pp. 283–316.
Wu. T. M, Yen. S. J, Chen. E. C, Chiang. R. K, Journal of Polymer Science: Part B: Polymer Physics, Vol. 46, 727-733, 2008.
Y. Kurokawa, Y. Hosoya, Surface, 34(2) 100-106 (1996).
Yaacob, I. I, S. Bhandarkar, and A. Bose, J Mater. Research, Vol. 8, No. 3, 1993, pp. 573–577.
Yarwood. J, Analyt. Proc., Vol. 30, 1993, pp. 13–18.

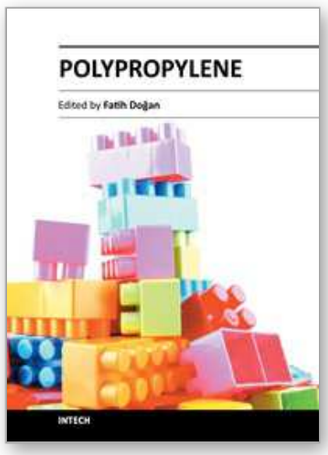

Polypropylene

Edited by Dr. Fatih Dogan

ISBN 978-953-51-0636-4
Hard cover, 500 pages
Publisher InTech
Published online 30, May, 2012
Published in print edition May, 2012

This book aims to bring together researchers and their papers on polypropylene, and to describe and illustrate the developmental stages polypropylene has gone through over the last 70 years. Besides, one can find papers not only on every application and practice of polypropylene but also on the latest polypropylene technologies. It is also intended in this compilation to present information on polypropylene in a medium readily accessible for any reader.

How to reference

In order to correctly reference this scholarly work, feel free to copy and paste the following:

Alireza Aslani (2012). Organic Materials in Nanochemistry, Polypropylene, Dr. Fatih Dogan (Ed.), ISBN: 978-953-51-0636-4, InTech, Available from: http://www.intechopen.com/books/polypropylene/organic-materials-in-nanochemistry

INTECH
open science | open minds

InTech Europe
University Campus STeP Ri
Slavka Krautzeka 83/A
51000 Rijeka, Croatia
Phone: +385 (51) 770 447
Fax: +385 (51) 686 166
www.intechopen.com

InTech China
Unit 405, Office Block, Hotel Equatorial Shanghai
No.65, Yan An Road (West), Shanghai, 200040, China
中国上海市延安西路65号上海国际贵都大饭店办公楼405单元
Phone: +86-21-62489820
Fax: +86-21-62489821

IntechOpen